Minimizing Hydraulic Resistance of a Plant Root

by

Shape Optimization

by

Sriram Chandrashekar

A Thesis Presented in Partial Fulfillment
of the Requirements for the Degree
Master of Science

Approved July 2016 by the
Graduate Supervisory Committee:

Kangping Chen, Chair
Konrad Rykaczewski
Huei-Ping Huang

ARIZONA STATE UNIVERSITY

August 2016

ABSTRACT

Analytical solution of the pressure field for water uptake through a composite root, coupled with fully saturated soil is derived by using the slender body approximation. It is shown that in general, the resistance of the root and soil are not additive. This result can play a very important role in modelling water uptake through plant roots and determination of hydraulic resistances of plant roots. Optimum plant root structure that minimizes a single root's hydraulic resistance is also studied in this work with the constraint of prescribed root volume. Hydraulic resistances under the slender body approximation and without such a limitation are considered. It is found that for large stele-to-cortex permeability ratio, there exists an optimum root length-to-base-radius ratio that minimizes the hydraulic resistance. A remarkable feature of the optimum root structure is that the optimum dimensionless stele conductivity depends only on a single geometrical parameter, the stele-to-root base-radius ratio. Once the stele-to-root base-radius ratio and the stele-to-cortex permeability ratio are given, the optimum root length-to-radius ratio can be found. While these findings remain to be verified by experiments for real plant roots, they offer theoretical guidance for the design of bio-inspired structures that minimizes hydraulic resistance for fluid production from porous media.

ACKNOWLEDGMENTS

I would like to sincerely thank Dr. Chen, my thesis advisor, for the encouragement and support that he has provided at every step and for being a great teacher.

I would like to thank Dr. Konrad Rykaczewski for being part of my thesis committee and the invaluable experience gained during my time as a research assistant in his research group.

I would also like to thank Dr. Huei-Ping Huang for being part of my thesis committee and for one of the best classes on Engineering Mathematics that has played an integral part of my research work.

TABLE OF CONTENTS

Page

LIST OF FIGURES

Figure Page

1. Introduction

The need for a quantitative expression of water uptake through plant roots is a problem of key importance to plant biology and ecology. Water-uptake from soil by a plant's root system has been studied extensively during the past seven decades (Philip, 1957; Gardner, 1960; Cowan, 1965; Landsberg & Fowkes, 1978; Molz, 1981; Passioura, 1988; Steudle & Peterson, 1998; Doussan et al., 1998; Steudle, 2000; Raats, 2007; Roose & Schnepf, 2008; Stroock et al., 2014). A single root has been historically modelled as an infinitely long porous cylinder with a two dimensional radial flow around the cylindrical root (Gardner, 1960; Landsberg & Fowkes, 1978; Ratts, 2007). In this model, the flow inside the stele is modelled to be one dimensional, along the root's axial direction since the flow through the stele and further onto the plant is dictated by xylem tubes that are aligned along the axis of the stele. Outside the stele, the flow is modelled to be purely in the radial direction, perpendicular to the axis of the stele.

It is important to consider the macroscopic root system and its relation to the water uptake calculation of a single root. The differential equation at the macroscopic level that governs the flow of water in the soil which is coupled to water-uptake by a root system, known as the Richard's equation (Raats, 2007), is given by

$$\frac{\partial \theta}{\partial t} = \nabla \cdot [K \nabla p] - S$$

where θ is the volumetric water content (or relative water saturation; moisture content); $K = K(\theta)$ is the conductivity in the soil which depends on the local water content; p is the water pressure in the soil pores which is also linked to the local water content, $p = p(\theta)$;

and S is a volumetric sink term representing root water-uptake. The term S is of extreme importance as it represents the water uptake and one way to model it is

$$S = N(\mathbf{x})\frac{p(\theta) - p_r(\mathbf{x})}{R}$$

where $N(\mathbf{x})$ is the root density distribution (number of root per unit soil volume); R is the single root hydraulic resistance; $p(\theta) - p_r(\mathbf{x})$ is the difference between the water pressure in the soil and the water pressure in the root; and $\left(p(\theta) - p_r(\mathbf{x})\right)/R$ is the water-uptake by a single root. The term R represents the hydraulic resistance of a single root and is the ratio of pressure drop across the root divided by the flow rate at the base of the stele. The determination of this resistance requires knowledge of the flow field in a single root.

Raats (2007) has discussed the various models used for modelling plant roots and all these models are variations of the basic model formulated by Gardner (1960). The above mentioned model of a two-dimensional flow has serious limitations, because in reality, the finite length of a root causes the flow around the root tip to be locally three-dimensional and the large flux near the tip makes a significant contribution to the water-uptake rate which the Gardner model fails to capture.

To account for this three dimensionality of the flow, Chen (2015) modelled the root as a slender semi-prolate spheroid consisting of a single uniform structure, the stele. This configuration yielded an analytical solution in terms of Legendre polynomials and the resulting flow field is three-dimensional near the tip of the root and shows a converging flow field close to the tip. This work also showed that by not considering the finite length of the root and the resulting three dimensional flow, the Gardner (1960) model under-

predicts the flow rate in comparison to the model proposed by Chen (2015). The physics of the resulting flow field is discussed in detail by Chen (2015).

The hydraulic resistance, which is a key part of the volumetric term S, is the ratio of pressure drop across the root to the flow rate through the base of the stele. The under-prediction by the cylindrical model results in a higher computed resistance of the root. In view of this, a new formula for the computation of root resistance is offered by Chen (2016), by considering a semi-prolate spheroidal geometry for the root and specifying a constant pressure (labelled P_1 in this work) at the root-soil surface. The root is modelled to consist of an inner stele in which the flow is assumed to be one-dimensional and an outer cortex. The resistance is then calculated as the ratio of the pressure difference between the root-soil surface pressure and the pressure at the base of the stele, to the volumetric flow rate in the stele. In the composite root model of Chen (2016), the flux from the cortex to the stele has a singularity close to the tip of the stele and this is due to the same physics that cause the flow from the soil to a single root to have a singularity at the root tip, as discussed by Chen (2015).

It is commonly believed in the plant biology community that the hydraulic resistance is additive, using such analogy as electric resistance in serial, i.e. the resistance of the root and soil system is the sum of the resistance of the root and the resistance of the soil. However, we show in this study that, in general, the resistance of the combined root and soil system does not equal the sum of individual resistances of the root and soil. This result can play a key role in future modelling of water uptake in plants since, a flow governed by a linear law does not necessarily give a linear relation for the resistances when the flow is not one-dimensional.

This is shown by coupling the composite root system of stele and cortex with the soil to form an extended domain and specifying a constant pressure P_e at the outer edge of this domain and a pressure P_w at the base of the stele ($P_w < P_1 < P_e$). Now, the resistance of the combined soil and root system would be given by the difference between P_e and P_w divided by the flow rate at the base of the stele.

The soil resistance is computed by considering the region of soil bounded by the outer ellipsoidal constant pressure boundary and the inner confocal soil-root boundary. A constant pressure P_1 is imposed on the root-soil interface. The flow rate through the soil for this configuration is then computed and used to calculate the resistance of the soil.

The hydraulic resistance of the root is then calculated by computing the flow rate through the composite root with the constant pressure P_1 imposed on the root soil surface. This formula was derived by Chen (2016) as mentioned earlier and is adopted for the computation of the hydraulic resistance.

It is then shown that the resistance of the coupled system is not equal to the sum of the resistances of the soil and root. For the coupled composite root and soil system solved in this work, we find that the pressure along the cortex soil interface is not a constant for finite values of dimensionless root conductivity and therefore adding the separate resistances of soil and the composite resistances yields wrong results, since the fluid flow in the soil is not hydrodynamically coupled to the fluid flow in the root. As the dimensioneless root conductivity becomes infinitely large however, we find that the pressure on the root-soil interface becomes constant and under this limit, the resistances are additive.

The dependence the hydraulic resistance of the root, obtained by Chen (2016), on the root shape is also studied by considering the dependence of resistance on the length-to-base radius ratio of the root. At constant values of the dimensionless stele conductivity, the resistance decreases continuously when the length to-base radius ratio of the root is increased. It is also seen that for a given value of permeability ratio λ, there exists an optimum length-to-base radius ratio which minimizes the hydraulic resistance. This optimum length-to-base radius ratio corresponds to a constant value of the stele dimensionless conductivity which is independent of the cortex-to-stele permeability ratio. The optimum stele dimensionless conductivity, however, depends on the volume fraction of the stele.

For the purpose of this study, the soil is assumed to be completely saturated at all times and a steady state problem is solved. At the moment, the discussion does not involve a time varying problem.

2. Mathematical formulation

The system under consideration is a root with a composite structure of a stele and cortex surrounded by completely saturated soil. The soil saturation is considered to be independent of time for this analysis. The composite root is taken to consist of an outer cortex and an inner stele (or xylem) with permeablities κ_c and κ_x respectively. The stele and the root are modelled as confocal spheroids and the soil outer boundary is also an ellipsoid, confocal to the ellipsoidal surfaces representing the complex root. This surface is taken to be at a constant pressure and the soil permeability represented by κ_s (Fig. 1).

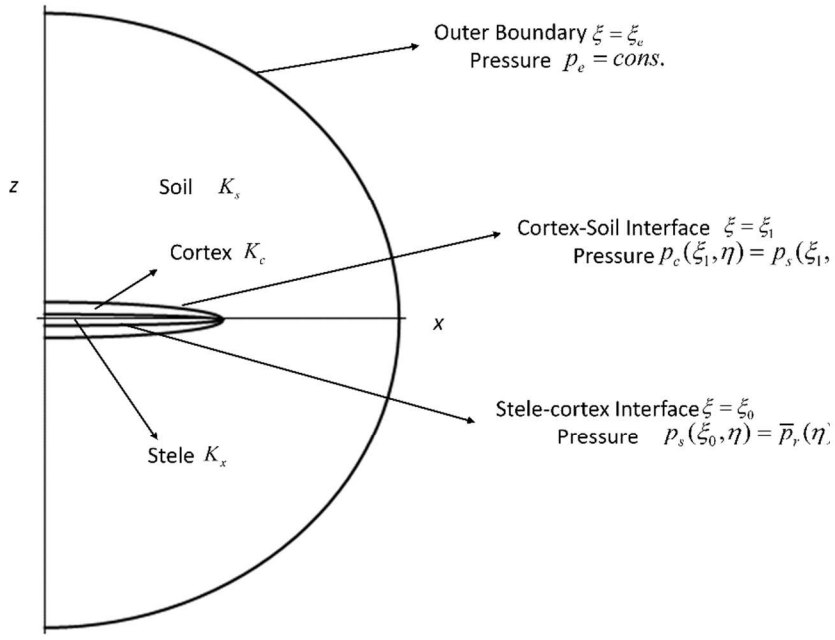

FIGURE 1. Prolate spheroidal modelling of a composite root in a saturated region of soil.

The flow along the stele is modelled as one-dimensional with the pressure being a function of only one ellipsoidal co-ordinate ($\tilde{\eta}$). The prolate ellipsoidal co-ordinates are given by $\tilde{\xi},\tilde{\eta},\tilde{\varphi}$. Here, surfaces corresponding to constant values of $\tilde{\xi}$ represent confocal ellipsoids, surfaces corresponding to constant values of $\tilde{\eta}$ represent confocal hyperboloids and $\tilde{\varphi}$ represents the azimuthal angle. The prolate ellipsoidal co-ordinates are related to the Cartesian co-ordinates by the following transformations

$$\begin{aligned} x &= \cosh\tilde{\xi}\cos\tilde{\eta} \\ y &= \sinh\tilde{\xi}\sin\tilde{\eta}\sin\tilde{\varphi} \\ z &= \sinh\tilde{\xi}\sin\tilde{\eta}\cos\tilde{\varphi} \end{aligned} \tag{1}$$

The stele-cortex interface is represented by the ellipsoidal surface corresponding to a constant $\tilde{\xi}_0$, the cortex-soil surface is represented by $\tilde{\xi}_1$ and the outer boundary of the soil is at $\tilde{\xi}_e$. The problem is axisymmetric about the x axis. Therefore no changes take place along the azimuthal direction $\tilde{\varphi}$ and all dependence on this co-ordinate is neglected.

At the outer boundary in the soil corresponding to $\tilde{\xi}_e$ a constant pressure P_e is specified while at the base of the stele (which corresponds to $\tilde{\eta}=\frac{\pi}{2}$), a constant pressure of P_w is provided. In the following section, the differential equations for different sections of the domain are derived.

3. The Differential equations

3.1 Differential Equation in the Soil ($\tilde{\xi}_1 \le \tilde{\xi} \le \tilde{\xi}_e$)

The equation of continuity for a steady incompressible flow is

$$\nabla . \vec{\mathrm{v}} = 0$$

The flow of a fluid in a porous medium obeys Darcy's law and is given by

$$\vec{\mathrm{v}} = -\frac{\kappa}{\mu}\nabla P \tag{2}$$

Where κ represents the intrinsic permeability of the medium, μ represents the dynamic viscosity of the fluid, $\vec{v}$ represents the fluid velocity and P is the pressure at given point. When written as the components in the respective prolate spheroidal co-ordinates, we get

$$\mathrm{v}_{\tilde{\xi}} = -\frac{\kappa}{\mu}\frac{1}{h_{\tilde{\xi}}}\frac{\partial P}{\partial \tilde{\xi}} \tag{3}$$

$$\mathrm{v}_{\tilde{\eta}} = -\frac{\kappa}{\mu}\frac{1}{h_{\tilde{\eta}}}\frac{\partial P}{\partial \tilde{\eta}} \tag{4}$$

and $\mathrm{v}_{\tilde{\varphi}} = 0$ since the problem is axisymmetric about the x-axis. Here $h_{\tilde{\xi}}$ and $h_{\tilde{\eta}}$ corresponds to the scale factors of these two co-ordinates and are given by

$$h_{\tilde{\xi}} = h_{\tilde{\eta}} = L\sqrt{\sinh^2\tilde{\xi} + \sin^2\tilde{\eta}} \tag{5}$$

$$h_{\tilde{\varphi}} = L\sinh\tilde{\xi}\sin\tilde{\eta} \tag{6}$$

And L represents the focal length. When Darcy's law is substituted into the continuity equation for constant κ and μ , the pressure equation becomes

$$\nabla^2 P = 0$$

If the pressure in the soil is denoted by p_s , the above equation is expanded in prolate ellipsoidal co-ordinates as

$$\frac{\partial}{\partial \tilde{\xi}}\left(\frac{h_{\tilde{\eta}} h_{\tilde{\varphi}}}{h_{\tilde{\xi}}}\frac{\partial p_s}{\partial \tilde{\xi}}\right)+\frac{\partial}{\partial \tilde{\eta}}\left(\frac{h_{\tilde{\varphi}} h_{\tilde{\xi}}}{h_{\tilde{\eta}}}\frac{\partial p_s}{\partial \tilde{\eta}}\right)=0 \tag{7}$$

When the expressions for the scaling factors are substituted, we get

$$\frac{\partial}{\partial \tilde{\xi}}\left(L\sinh\tilde{\xi}\sin\tilde{\eta}\frac{\partial p_s}{\partial \tilde{\xi}}\right)+\frac{\partial}{\partial \tilde{\eta}}\left(L\sinh\tilde{\xi}\sin\tilde{\eta}\frac{\partial p_s}{\partial \tilde{\eta}}\right)=0 \tag{8}$$

Here, the problem is transformed to a new set of co-ordinates ξ,η,φ and these are related to the prolate spheroidal co-ordinates by the following relation

$$\begin{aligned}\xi &= \cosh\tilde{\xi}\\ \eta &= \cos\tilde{\eta}\\ \varphi &= \tilde{\varphi}\end{aligned} \tag{9}$$

Substituting these relations and dividing by $L\sinh\tilde{\xi}\sin\tilde{\eta}$ gives

$$\frac{\partial}{\partial \xi}\left((\xi^2-1)\frac{\partial p_s}{\partial \xi}\right)+\frac{\partial}{\partial \tilde{\eta}}\left((1-\eta^2)\frac{\partial p_s}{\partial \eta}\right)=0 \tag{10}$$

The solution for the above equation is discussed in Section 4.

3.2 Differential Equation in the Cortex ($\tilde{\xi}_0 \le \tilde{\xi} \le \tilde{\xi}_1$)

The flow in the cortex is similar to the flow in a soil except that it has a different permeability. Similar to the soil, the differential equation for the pressure in the cortex (p_c) is

$$\frac{\partial}{\partial \xi}\left((\xi^2 - 1)\frac{\partial p_c}{\partial \xi} \right) + \frac{\partial}{\partial \eta}\left((1-\eta^2)\frac{\partial p_c}{\partial \eta} \right) = 0 \tag{11}$$

3.3 Differential Equation in the Stele ($0 \le \tilde{\xi} \le \tilde{\xi}_0$)

The flow along the stele satisfies the continuity equation and in prolate ellipsoidal co-ordinates, this is given by

$$\frac{\partial (h_{\tilde{\eta}} h_{\tilde{\varphi}} v_{\tilde{\xi}})}{\partial \tilde{\xi}} + \frac{\partial (h_{\tilde{\varphi}} h_{\tilde{\xi}} v_{\tilde{\eta}})}{\partial \tilde{\eta}} = 0 \tag{12}$$

Multiply by 2π and integrate with respect to $\tilde{\xi}$ from 0 to $\tilde{\xi}_0$ to get

$$\frac{dq_r}{d\tilde{\eta}} + 2\pi \left(\mathrm{v}_{\tilde{\xi}} h_{\tilde{\eta}} h_{\tilde{\varphi}} \right) \Big|_0^{\tilde{\xi}_0} = 0 \tag{13}$$

where

$$q_r = 2\pi \int_0^{\tilde{\xi}_0} \mathrm{v}_{\tilde{\eta}} h_{\tilde{\varphi}} h_{\tilde{\xi}} d\tilde{\xi} \tag{14}$$

is the volumetric flow rate across a hyperboloid cross section corresponding to a constant value of $\tilde{\eta}$.

The flow is symmetric along the axis. Therefore at $\tilde{\xi} = 0$: $\mathrm{v}_{\tilde{\xi}} = 0$ and we get

$$\frac{dq_r}{d\tilde{\eta}} + 2\pi\left(\mathrm{v}_{\tilde{\xi}} h_{\tilde{\eta}} h_{\tilde{\varphi}}\right)\Big|_{\tilde{\xi}_0} = 0 \tag{15}$$

We can use Darcy's law to write the flow rate as

$$q_r = 2\pi\int_0^{\tilde{\xi}_0} \mathrm{v}_{\tilde{\eta}} h_{\tilde{\varphi}} h_{\tilde{\xi}} d\tilde{\xi} = -\frac{2\pi\kappa_x}{\mu}\int_0^{\tilde{\xi}_0} \frac{h_{\tilde{\varphi}} h_{\tilde{\xi}}}{h_{\tilde{\eta}}} \frac{\partial p_r}{\partial \tilde{\eta}} d\tilde{\xi} = -\frac{2\pi\kappa_x}{\mu} L \sin\tilde{\eta} \frac{\partial}{\partial \tilde{\eta}}\int_0^{\tilde{\xi}_0} p_r \sinh\tilde{\xi} d\tilde{\xi} \tag{16}$$

A cross sectional averaged root pressure is written as

$$\overline{p}_r = \frac{2\pi\int_0^{\tilde{\xi}_0} p_r h_{\tilde{\varphi}} h_{\tilde{\xi}} d\tilde{\xi}}{A_{\tilde{\xi}}} \tag{17}$$

And

$$A_{\tilde{\xi}} = 2\pi\int_0^{\tilde{\xi}_0} h_{\tilde{\varphi}} h_{\tilde{\xi}} d\tilde{\xi} = 2\pi L^2 \sin^2\tilde{\eta}\left(\cosh\tilde{\xi}_0 - 1\right) \tag{18}$$

Also

$$2\pi\int_0^{\tilde{\xi}_0} p_r h_{\tilde{\varphi}} h_{\tilde{\xi}} d\tilde{\xi} = 2\pi L^2 \sin^2\tilde{\eta}\int_0^{\tilde{\xi}_0} p_r \sinh\tilde{\xi} d\tilde{\xi} \tag{19}$$

And the averaged pressure is

$$\bar{p}_r = \frac{\int_0^{\tilde{\xi}_0} p_r \sinh\tilde{\xi} d\tilde{\xi}}{\cosh\tilde{\xi}_0 - 1} \tag{20}$$

The volumetric flow rate (16) can therefore be expressed as

$$q_r = -\frac{2\pi\kappa_x}{\mu} L\left(\cosh\tilde{\xi}_0 - 1\right)\sin\tilde{\eta}\frac{d\bar{p}_r}{d\tilde{\eta}} \tag{21}$$

Substituting (21) into (15) gives

$$\frac{\kappa_r}{\mu} L\left(\cosh\tilde{\xi}_0 - 1\right)\frac{d}{d\tilde{\eta}}\left(\sin\tilde{\eta}\frac{d\bar{p}_r}{d\tilde{\eta}}\right) - \left(\mathrm{v}_{\tilde{\xi}} h_{\tilde{\eta}} h_{\tilde{\phi}}\right)\Big|_{\tilde{\xi}_0} = 0 \tag{22}$$

The velocity component $\mathrm{v}_{\tilde{\xi}}$ is continuous at the root surface $\tilde{\xi} = \tilde{\xi}_0$, and $\mathrm{v}_{\tilde{\xi}}$ from the cortex side at the root surface is (after applying Darcy's law),

$$(\mathrm{v}_{\tilde{\xi}}\mathrm{h}_{\tilde{\eta}}\mathrm{h}_{\tilde{\phi}})\,|_{\tilde{\xi}_0} = -\frac{\kappa_c}{\mu}\frac{\mathrm{h}_{\tilde{\eta}}\mathrm{h}_{\tilde{\phi}}}{h_{\tilde{\xi}}}\frac{\partial p_c}{\partial\tilde{\xi}}|_{\tilde{\xi}_0} = -\frac{\kappa_c}{\mu} L\sinh^2\tilde{\xi}_0\sin\tilde{\eta}\frac{\partial p_c}{\partial\xi}|_{\xi_0}\ , \tag{23}$$

where we have used $\xi = \cosh\tilde{\xi}$ to transform the derivative $\frac{\partial p_c}{\partial\tilde{\xi}}$ to $\frac{\partial p_c}{\partial\xi}$. Thus, the equation. for the average pressure inside the stele becomes

$$\frac{\kappa_x}{\mu} L(\cosh\tilde{\xi}_0 - 1)\frac{d}{d\tilde{\eta}}(\sin\tilde{\eta}\frac{d\bar{p}_r}{d\tilde{\eta}}) + \frac{\kappa_c}{\mu} L\sinh^2\tilde{\xi}_0\sin\tilde{\eta}\frac{\partial p_c}{\partial\xi}|_{\xi_0} = 0\,, \tag{24}$$

which can be re-written as

$$\frac{\lambda}{\xi_0 + 1}\frac{d}{d\tilde{\eta}}(\sin\tilde{\eta}\frac{d\bar{p}_r}{d\tilde{\eta}}) + \sin\tilde{\eta}\frac{\partial p_c}{\partial\xi}|_{\xi_0} = 0\ , \tag{25}$$

where $\lambda = \frac{\kappa_x}{\kappa_c}$ is the ratio between the stele permeability and the cortex permeability.

4. Solutions of the differential equations

4.1 Solution in the soil ($\xi_1 \le \xi \le \xi_e$)

The technique of separation of variables is used to solve the differential equation (10) in the soil.

Let

$$p_s(\xi,\eta) = F(\xi)G(\eta) \tag{26}$$

This gives

$$\frac{d}{d\xi}\left[(1-\xi^2)\frac{dF}{d\xi}\right] + \chi F = 0, 1 \le \xi < \infty \tag{27}$$

$$\frac{d}{d\eta}\left[(1-\eta^2)\frac{dG}{d\eta}\right] + \chi G = 0, 0 \le \eta \le 1 \tag{28}$$

F and G satisfy the same differential equation but their arguments lie in different ranges. This is the Legendre differential equation. For $G(\eta)$, it has to be finite at $\eta = 1$, since $p_s(\xi,\eta)$ is finite at $\eta = 1$ ($\tilde{\eta} = 0$). Thus, the eigenvalue χ has to be

$$\chi = n(n+1),\ n = 0,1,2....$$

and

$$G(\eta) = P_n(\eta)$$

where $P_n(\eta)$ are the Legendre polynomials. The polynomials are odd functions for odd values of n and even functions for even values of n . Since $p_s(\xi,\eta)$ is also symmetric about $\eta = 1, 0$ ($\tilde{\eta} = 0, \pi/2$), $G(\eta)$ has to be an even function of $\tilde{\eta}$ .Thus, we have $n = 2m,\ m = 0,1,2....$. Therefore,

$$G(\eta) = P_{2m}(\eta),\ m = 0,1,2,....$$

The solution for $F(\xi)$ is a combination of the zeroth-order associated Legendre function of the first kind and the second kind, P_{2m} and Q_{2m}, respectively, of the even order (ξ has a different range, and Q_{2m} are not polynomials):

$$F(\xi) = A_{2m}P_{2m}(\xi) + B_{2m}Q_{2m}(\xi) \tag{29}$$

A particular solution for any value of m is given by

$$p_s(\xi,\eta) = [\mathrm{A}_{2m}\mathrm{P}_{2m}(\xi) + \mathrm{B}_{2m}\mathrm{Q}_{2m}(\xi)]P_{2m}(\eta)$$

Since we have a linear differential equation for $p_s(\xi,\eta)$, the general solution is a linear combination of particular solutions and is given by

$$p_s(\xi,\eta) = \sum_{m=0}^{\infty}[\mathrm{A}_{2m}\mathrm{P}_{2m}(\xi) + \mathrm{B}_{2m}\mathrm{Q}_{2m}(\xi)]P_{2m}(\eta) \tag{30}$$

4.2 Solution for the cortex ($\xi_0 \le \xi \le \xi_1$)

Since the flow through the cortex satisfies the same differential equation as the soil, with the same range of η but ξ from ξ_0 to ξ_1, we have

$$p_c(\xi,\eta) = \sum_{m=0}^{\infty}[\mathrm{C}_{2m}\mathrm{P}_{2m}(\xi) + D_{2m}\,\mathrm{Q}_{2m}(\xi)]P_{2m}(\eta) \tag{31}$$

Which has the same form as (30) for the soil, with different co-efficients.

4.3 Solution in the stele ($1 \le \xi \le \xi_0$)

From (25) the pressure equation inside the stele is

$$\frac{\lambda}{\xi_0+1}\frac{d}{d\tilde{\eta}}(\sin\tilde{\eta}\frac{d\overline{p}_r}{d\tilde{\eta}})+\sin\tilde{\eta}\frac{\partial p_c}{\partial\xi}|_{\xi_0}=0$$

Notice that

$$\eta=\cos\tilde{\eta}$$

$$\frac{d}{d\tilde{\eta}}=\frac{d}{d\eta}\frac{d\eta}{d\tilde{\eta}}=-\sin\tilde{\eta}\frac{d}{d\eta}$$

$$\frac{d}{d\tilde{\eta}}\left(\sin\tilde{\eta}\frac{d\overline{p}_r}{d\tilde{\eta}}\right)=\sin\tilde{\eta}\frac{d}{d\eta}\left[\left(1-\eta^2\right)\frac{d\overline{p}_r}{d\eta}\right]$$

The pressure equn. can be transformed to

$$\frac{\lambda}{\xi_0+1}\frac{d}{d\eta}\left[\left(1-\eta^2\right)\frac{d\overline{p}_r}{d\eta}\right]+\left.\frac{\partial p_c}{\partial\xi}\right|_{\xi_0}=0 \qquad (32)$$

From the pressure solution in the cortex, (31), we have

$$\left.\frac{\partial p_c}{\partial\xi}\right|_{\xi_0}=\sum_{m=0}^{\infty}\left[C_{2m}P_{2m}^{'}(\xi_0)+D_{2m}Q_{2m}^{'}(\xi_0)\right]P_{2m}(\eta)$$

$$=D_0Q_0^{'}(\xi_0)+\sum_{m=1}^{\infty}\left[C_{2m}P_{2m}^{'}(\xi_0)+D_{2m}Q_{2m}^{'}(\xi_0)\right]P_{2m}(\eta)$$

$P_{2m}(\eta)$ satisfies the Legendre differential equation

$$\frac{d}{d\eta}\left[(1-\eta^2)\frac{dP_{2m}(\eta)}{d\eta}\right]+2m(2m+1)P_{2m}(\eta)=0,\ m=0,1,2,....$$

Thus,

$$P_{2m}(\eta)=-\frac{1}{2m(2m+1)}\frac{d}{d\eta}\left[(1-\eta^2)\frac{dP_{2m}(\eta)}{d\eta}\right],\ m\geq 1$$

Equation. (32) can be re-written as

$$\frac{d}{d\eta}[(1-\eta^2)\frac{d\overline{p}_r}{d\eta}]+$$
$$\frac{\xi_0+1}{\lambda}\{\mathrm{D}_0\mathrm{Q}_0'(\xi_0)-\sum_{m=1}^{\infty}\frac{C_{2m}P_{2m}'(\xi_0)+D_{2m}Q_{2m}'(\xi_0)}{2m(2\,\mathrm{m}+1)}\frac{d}{d\eta}[(1-\eta^2)\frac{dP_{2m}(\eta)}{d\eta}]\}=0 \tag{33}$$

Integrate this equation once, to obtain

$$(1-\eta^2)\frac{d\overline{p}_r}{d\eta}+\frac{\xi_0+1}{\lambda}\{\mathrm{D}_0\mathrm{Q}_0'(\xi_0)\eta-$$
$$\sum_{m=1}^{\infty}\frac{C_{2m}P_{2m}'(\xi_0)+D_{2m}Q_{2m}'(\xi_0)}{2m(2\,\mathrm{m}+1)}(1-\eta^2)\frac{dP_{2m}(\eta)}{d\eta}\}=c_1\frac{\xi_0+1}{\lambda}\ , \tag{34}$$

where c_1 is an integration constant. (34) can be re-arranged to

$$\frac{d\overline{p}_r}{d\eta}$$
$$-\frac{\xi_0+1}{\lambda}\sum_{m=1}^{\infty}\frac{C_{2m}P_{2m}'(\xi_0)+D_{2m}Q_{2m}'(\xi_0)}{2m(2\,\mathrm{m}+1)}\frac{dP_{2m}(\eta)}{d\eta}=\frac{\xi_0+1}{\lambda}\frac{(c_1-\mathrm{D}_0\mathrm{Q}_0'(\xi_0)\eta)}{(1-\eta^2)}\ . \tag{35}$$

Notice that the symmetric condition

$$\left.\frac{d\overline{p}_r}{d\tilde{\eta}}\right|_{\tilde{\eta}=0}=0$$

is always satisfied by virtue of

$$\left.\frac{d\overline{p}_r}{d\tilde{\eta}}\right|_{\tilde{\eta}=0}=-\left.\frac{d\overline{p}_r}{d\eta}\right|_{\eta=1}\sin\tilde{\eta}\big|_{\tilde{\eta}=0}=0$$

as long as pressure gradient $\frac{d\overline{p}_r}{d\eta}$ is finite at $\eta=1$. From (35), this latter requirement makes it necessary that

$$c_1=\mathrm{D}_0\mathrm{Q}_0'(\xi_0) \tag{36}$$

such that (35) becomes

$$\frac{d\bar{p}_r}{d\eta} - \frac{\xi_0+1}{\lambda}\sum_{m=1}^{\infty}\frac{C_{2m}P_{2m}'(\xi_0)+D_{2m}Q_{2m}'(\xi_0)}{2m(2\mathrm{m}+1)}\frac{dP_{2m}(\eta)}{d\eta} = \frac{\xi_0+1}{\lambda}\frac{\mathrm{D}_0\mathrm{Q}_0'(\xi_0)}{(1+\eta)} \quad . (37)$$

A further integration gives the pressure inside the stele as

$$\bar{p}_r = c_2 + \frac{\xi_0+1}{\lambda}\mathrm{D}_0\mathrm{Q}_0'(\xi_0)\ln(1+\eta) + \frac{\xi_0+1}{\lambda}\sum_{m=1}^{\infty}\frac{C_{2m}P_{2m}'(\xi_0)+D_{2m}Q_{2m}'(\xi_0)}{2m(2\mathrm{m}+1)}P_{2m}(\eta)$$

. (38)

c_2 is an integration constant. The boundary condition at the base of the root can be used to determine c_2:

$$\tilde{\eta} = \pi/2 (\eta = \cos\tilde{\eta} = 0) : \bar{p}_r = p_w$$

Thus

$$c_2 = \bar{p}_w - \frac{\xi_0+1}{\lambda}\sum_{m=1}^{\infty}\frac{C_{2m}P_{2m}'(\xi_0)+D_{2m}Q_{2m}'(\xi_0)}{2m(2\mathrm{m}+1)}P_{2m}(0) \quad (39)$$

The pressure inside the stele is then given by

$$\bar{p}_r = \bar{p}_w - \frac{\xi_0+1}{\lambda}\sum_{m=1}^{\infty}\frac{C_{2m}P_{2m}'(\xi_0)+D_{2m}Q_{2m}'(\xi_0)}{2m(2\mathrm{m}+1)}P_{2m}(0)$$
$$+\frac{\xi_0+1}{\lambda}\mathrm{D}_0\mathrm{Q}_0'(\xi_0)\ln(1+\eta) + \frac{\xi_0+1}{\lambda}\sum_{m=1}^{\infty}\frac{C_{2m}P_{2m}'(\xi_0)+D_{2m}Q_{2m}'(\xi_0)}{2m(2\mathrm{m}+1)}P_{2m}(\eta)$$

(40)

5. Determination of the Coefficients

Determination the coefficients A_{2m}, B_{2m}, C_{2m} and D_{2m} requires the use of boundary conditions. For the soil, these are

$$\xi = \xi_e : p_s = p_e \quad (\textit{constant outer boundary pressure in the soil}) \tag{41}$$

$$\xi = \xi_1 : p_s(\xi_1, \eta) = p_c(\xi_1, \eta) \quad (\textit{equal pressure at the soil-cortex interface}) \tag{42}$$

$$\xi = \xi_1 : \kappa_s \frac{\partial p_s}{\partial \xi}|_{\xi_1} = \kappa_c \frac{\partial p_c}{\partial \xi}|_{\xi_1} \quad (\textit{equal velocity } v_{\tilde{\xi}} \textit{ at the soil-cortex interface}) \tag{43}$$

Using the first boundary condition, (and noting that for any variable, $P_0(x) = 1$), gives

$$A_0 + B_0 Q_0(\xi_e) = p_e \ , \tag{44}$$

$$A_{2m} P_{2m}(\xi_e) + B_{2m} Q_{2m}(\xi_e) = 0 \ \ for \ \ m \geq 1 \tag{45}$$

The second boundary condition and using the solution for the pressure field in the cortex, at $\xi = \xi_1$ gives

$$\sum_{m=0}^{\infty} [\mathrm{A}_{2m} \mathrm{P}_{2m}(\xi_1) + \mathrm{B}_{2m} \mathrm{Q}_{2m}(\xi_1)] P_{2m}(\eta) = \sum_{m=0}^{\infty} [\mathrm{C}_{2m} \mathrm{P}_{2m}(\xi_1) + D_{2m} \mathrm{Q}_{2m}(\xi_1)] P_{2m}(\eta) \ . \tag{46}$$

The third boundary condition gives

$$\kappa_s \sum_{m=0}^{\infty} [\mathrm{A}_{2m} \mathrm{P}_{2m}'(\xi_1) + \mathrm{B}_{2m} \mathrm{Q}_{2m}'(\xi_1)] P_{2m}(\eta) = \kappa_c \sum_{m=0}^{\infty} [\mathrm{C}_{2m} \mathrm{P}_{2m}'(\xi_1) + D_{2m} \mathrm{Q}_{2m}'(\xi_1)] P_{2m}(\eta)$$

. (47)

The Legendre Polynomials are orthogonal to each other and satisfy the following relation:

$$\int_{-1}^{1} P_k(\eta)P_l(\eta)\,\mathrm{d}\eta = \begin{cases} \dfrac{2}{2k+1}, k = l \\ 0, \qquad k \neq l \end{cases} \tag{48}$$

Applying the orthogonal condition to (46) and (47) gives

$$\mathrm{A}_{2m}\mathrm{P}_{2m}(\xi_1) + \mathrm{B}_{2m}\mathrm{Q}_{2m}(\xi_1) = \mathrm{C}_{2m}\mathrm{P}_{2m}(\xi_1) + D_{2m}\,\mathrm{Q}_{2m}(\xi_1) \tag{49}$$

$$\kappa_s[\mathrm{A}_{2m}\mathrm{P}_{2m}'(\xi_1) + \mathrm{B}_{2m}\mathrm{Q}_{2m}'(\xi_1)] = \kappa_c[\mathrm{C}_{2m}\mathrm{P}_{2m}'(\xi_1) + D_{2m}\,\mathrm{Q}_{2m}'(\xi_1)] \tag{50}$$

The boundary condition at the stele-cortex interface is

$$\xi = \xi_0 : p_c(\xi_0, \eta) = \overline{p}_r(\eta)\ , \tag{51}$$

which gives (after using the orthogonal property of Legendre Polynomials)

$$C_{2m}P_{2m}(\xi_0) + \mathrm{D}_{2m}\,Q_{2m}(\xi_0) = \frac{4m+1}{2}\int_{-1}^{1} \overline{p}_r(\eta)P_{2n}(\eta)d\eta \ \ for \ \ m = n \geq 0 \tag{52}$$

Therefore, to determine the coefficients, the relations are

For $m = 0$,

$$\kappa_c D_0 = \kappa_s B_0 \tag{53}$$

$$A_0 + B_0 Q_0(\xi_e) = p_e \tag{54}$$

$$C_0 - A_0 + Q_0(\xi_1)[\mathrm{D}_0 - \mathrm{B}_0] = 0 \tag{55}$$

$$C_0 + D_0 Q_0(\xi_0) = \int_0^1 \overline{p}_r(\eta)d\eta \tag{56}$$

For, $m \geq 1$

$$A_{2m}P_{2m}(\xi_e) + B_{2m}Q_{2m}(\xi_e) = 0 \tag{57}$$

$$A_{2m}P_{2m}(\xi_1) + B_{2m}Q_{2m}(\xi_1) = \mathrm{C}_{2m}\,P_{2m}(\xi_1) + \mathrm{D}_{2m}\,Q_{2m}(\xi_1) \tag{58}$$

$$\kappa_s[\,A_{2m}P_{2m}\,'(\xi_1) + B_{2m}Q_{2m}\,'(\xi_1)] = \kappa_c[\mathrm{C}_{2m}\,P_{2m}\,'(\xi_1) + \mathrm{D}_{2m}\,Q_{2m}\,'(\xi_1)] \tag{59}$$

$$C_{2m}P_{2m}(\xi_0) + \mathrm{D}_{2m}\,Q_{2m}(\xi_0) = \frac{4m+1}{2}\int_{-1}^{1}\overline{p}_r(\eta)P_{2n}(\eta)d\eta \tag{60}$$

(53) is re-written as

$$D_0 = \tau B_0 \tag{61}$$

where $\tau = \dfrac{\kappa_s}{\kappa_c}$ is the soil-to-cortex permeability ratio. Using this expression (54) is re-written as

$$A_0 = p_e - \frac{D_0}{\tau}Q_0(\xi_e) \tag{62}$$

(61) and (62) can be substituted into (55) to give

$$C_0 = p_e - \frac{D_0}{\tau}Q_0(\xi_e) - Q_0(\xi_1)[\mathrm{D}_0 - \frac{D_0}{\tau}] \tag{63}$$

Substituting (63) in (56) gives

$$p_e - \frac{D_0}{\tau}Q_0(\xi_e) - Q_0(\xi_1)[\mathrm{D}_0 - \frac{D_0}{\tau}] + D_0Q_0(\xi_0) = \int_0^1 \overline{p}_r(\eta)d\eta$$

which can then be re-arranged to read

$$D_0 = \frac{\int_0^1 \overline{p}_r(\eta)d\eta - p_e}{Q_0(\xi_0) - Q_0(\xi_1)[1 - \frac{1}{\tau}] - \frac{Q_0(\xi_e)}{\tau}}\ . \tag{64}$$

The integral in the numerator is evaluated as

$$\int_0^1 \bar{p}_r d\eta = \bar{p}_w \eta \,|_0^1 - [\frac{\xi_0 + 1}{\lambda} \sum_{m=1}^{\infty} \frac{C_{2m} P_{2m}'(\xi_0) + D_{2m} Q_{2m}'(\xi_0)}{2m(2\mathrm{m}+1)} P_{2m}(0)] \eta \,|_0^1$$
$$+ \frac{\xi_0 + 1}{\lambda} \mathrm{D}_0 \mathrm{Q}_0'(\xi_0)[(1+\eta)\ln(1+\eta) - \eta] \,|_0^1 \qquad (65)$$
$$+ \frac{\xi_0 + 1}{\lambda} \sum_{m=1}^{\infty} \frac{C_{2m} P_{2m}'(\xi_0) + D_{2m} Q_{2m}'(\xi_0)}{2m(2\mathrm{m}+1)} \int_0^1 P_{2m}(\eta) d\eta$$

It should be noted that for $m \geq 1$,

$$\int_0^1 P_{2m}(\eta) d\eta = 0 \qquad (66)$$

This results in

$$\int_0^1 \bar{p}_r d\eta = \bar{p}_w - \frac{\xi_0 + 1}{\lambda} \sum_{m=1}^{\infty} \frac{C_{2m} P_{2m}'(\xi_0) + D_{2m} Q_{2m}'(\xi_0)}{2m(2\mathrm{m}+1)} P_{2m}(0)$$
$$+ \frac{\xi_0 + 1}{\lambda} \mathrm{D}_0 \mathrm{Q}_0'(\xi_0)[2\ln 2 - 1] \qquad (67)$$

Substituting (67) in (64) gives

$$D_0 = \frac{-\Delta p - \frac{\xi_0 + 1}{\lambda} \sum_{m=1}^{\infty} \frac{C_{2m} P_{2m}'(\xi_0) + D_{2m} Q_{2m}'(\xi_0)}{2m(2\mathrm{m}+1)} P_{2m}(0) + \frac{\xi_0 + 1}{\lambda} \mathrm{D}_0 \mathrm{Q}_0'(\xi_0)[2\ln 2 - 1]}{Q_0(\xi_0) - Q_0(\xi_1)[1 - \frac{1}{\tau}] - \frac{Q_0(\xi_e)}{\tau}}$$

(68)

where $\Delta p = p_e - \bar{p}_w$

Eq (57) is now re-written as

$$A_{2m} = \frac{-B_{2m} Q_{2m}(\xi_e)}{P_{2m}(\xi_e)} \quad . \qquad (69)$$

Substituting this in (58) and re-arranging gives

$$\mathrm{C}_{2m} = B_{2m}[\frac{Q_{2m}(\xi_1)}{P_{2m}(\xi_1)} - \frac{Q_{2m}(\xi_e)}{P_{2m}(\xi_e)}] - \mathrm{D}_{2m}\frac{Q_{2m}(\xi_1)}{P_{2m}(\xi_1)} \ . \tag{70}$$

Sub (69) and (70) in (59) and re-arranging gives

$$B_{2m} = \mathrm{D}_{2m}\frac{[\frac{Q_{2m}'(\xi_1)}{P_{2m}'(\xi_1)} - \frac{Q_{2m}(\xi_1)}{P_{2m}(\xi_1)}]}{\tau[\frac{Q_{2m}'(\xi_1)}{P_{2m}'(\xi_1)} - \frac{Q_{2m}(\xi_e)}{P_{2m}(\xi_e)}] - [\frac{Q_{2m}(\xi_1)}{P_{2m}(\xi_1)} - \frac{Q_{2m}(\xi_e)}{P_{2m}(\xi_e)}]} \ . \tag{71}$$

Eq (60) reads

$$C_{2m}P_{2m}(\xi_0) + \mathrm{D}_{2m}Q_{2m}(\xi_0) = \frac{4m+1}{2}\int_{-1}^{1}\overline{p}_r(\eta)P_{2n}(\eta)d\eta \ \text{ for } \ m = n \geq 1$$

Which is re-arranged to

$$\mathrm{D}_{2m}Q_{2m}(\xi_0) = \frac{4m+1}{2}\int_{-1}^{1}\overline{p}_r(\eta)P_{2n}(\eta)d\eta - C_{2m}P_{2m}(\xi_0)$$

Substituting (70) for C_{2m} gives

$$\mathrm{D}_{2m}Q_{2m}(\xi_0) = \frac{4m+1}{2}\int_{-1}^{1}\overline{p}_r(\eta)P_{2n}(\eta)d\eta - \{B_{2m}[\frac{Q_{2m}(\xi_1)}{P_{2m}(\xi_1)} - \frac{Q_{2m}(\xi_e)}{P_{2m}(\xi_e)}] - \mathrm{D}_{2m}\frac{Q_{2m}(\xi_1)}{P_{2m}(\xi_1)}\}P_{2m}(\xi_0)$$

$$\mathrm{D}_{2m} = \frac{4m+1\int_{0}^{1}\overline{p}_r P_{2n}(\eta)d\eta}{\sigma_5(\tau,\xi_0,\xi_1,\xi_e)} \tag{72}$$

where

$$\begin{aligned}\sigma_5(\tau,\xi_0,\xi_1,\xi_e) = {} & \{\frac{Q_{2m}(\xi_0)}{P_{2m}(\xi_0)} - \frac{Q_{2m}(\xi_1)}{P_{2m}(\xi_1)}\}P_{2m}(\xi_0) \\ & + \frac{[\frac{Q_{2m}'(\xi_1)}{P_{2m}'(\xi_1)} - \frac{Q_{2m}(\xi_1)}{P_{2m}(\xi_1)}][\frac{Q_{2m}(\xi_1)}{P_{2m}(\xi_1)} - \frac{Q_{2m}(\xi_e)}{P_{2m}(\xi_e)}]P_{2m}(\xi_0)}{\tau[\frac{Q_{2m}'(\xi_1)}{P_{2m}'(\xi_1)} - \frac{Q_{2m}(\xi_e)}{P_{2m}(\xi_e)}] - [\frac{Q_{2m}(\xi_1)}{P_{2m}(\xi_1)} - \frac{Q_{2m}(\xi_e)}{P_{2m}(\xi_e)}]}\end{aligned} \tag{73}$$

Now the integral in (72) is evaluated as

$$\int_0^1 \overline{p}_r P_{2n}(\eta)d\eta = \frac{\xi_0+1}{\lambda}\mathrm{D}_0\mathrm{Q}_0'(\xi_0)\int_0^1 \ln(1+\eta)P_{2n}(\eta)d\eta + \frac{\xi_0+1}{\lambda}\frac{1}{4m+1}\frac{C_{2m}P_{2m}'(\xi_0)+D_{2m}Q_{2m}'(\xi_0)}{2m(2\,\mathrm{m}+1)} \quad . \tag{74}$$

Substituting (74) in (72) gives

$$\mathrm{D}_{2m} = \frac{(4m+1)\frac{\xi_0+1}{\lambda}\mathrm{D}_0\mathrm{Q}_0'(\xi_0)I_{2m} + \frac{\xi_0+1}{\lambda}\frac{C_{2m}P_{2m}'(\xi_0)+D_{2m}Q_{2m}'(\xi_0)}{2m(2\,\mathrm{m}+1)})}{\sigma_5(\tau,\xi_0,\xi_1,\xi_e)} \quad , \tag{75}$$

where

$$I_{2m} = \int_0^1 \ln(1+\eta)P_{2n}(\eta)d\eta .$$

Recall that (71) reads

$$\mathrm{C}_{2m} = B_{2m}[\frac{Q_{2m}(\xi_1)}{P_{2m}(\xi_1)} - \frac{Q_{2m}(\xi_e)}{P_{2m}(\xi_e)}] - \mathrm{D}_{2m}\frac{Q_{2m}(\xi_1)}{P_{2m}(\xi_1)} \quad .$$

Substituting for B_{2m} gives

$$\mathrm{C}_{2m} = \mathrm{D}_{2m}\frac{[\frac{Q_{2m}'(\xi_1)}{P_{2m}'(\xi_1)} - \frac{Q_{2m}(\xi_1)}{P_{2m}(\xi_1)}][\frac{Q_{2m}(\xi_1)}{P_{2m}(\xi_1)} - \frac{Q_{2m}(\xi_e)}{P_{2m}(\xi_e)}]}{\tau[\frac{Q_{2m}'(\xi_1)}{P_{2m}'(\xi_1)} - \frac{Q_{2m}(\xi_e)}{P_{2m}(\xi_e)}] - [\frac{Q_{2m}(\xi_1)}{P_{2m}(\xi_1)} - \frac{Q_{2m}(\xi_e)}{P_{2m}(\xi_e)}]} - \mathrm{D}_{2m}\frac{Q_{2m}(\xi_1)}{P_{2m}(\xi_1)} \quad ,$$

which can be re-written as

$$C_{2m} = \sigma_3(\tau,\xi_0,\xi_1,\xi_e)D_{2m} \quad , \tag{76}$$

with

$$\sigma_3(\tau,\xi_0,\xi_1,\xi_e) = \frac{[\frac{Q_{2m}'(\xi_1)}{P_{2m}'(\xi_1)} - \frac{Q_{2m}(\xi_1)}{P_{2m}(\xi_1)}][\frac{Q_{2m}(\xi_1)}{P_{2m}(\xi_1)} - \frac{Q_{2m}(\xi_e)}{P_{2m}(\xi_e)}]}{\tau[\frac{Q_{2m}'(\xi_1)}{P_{2m}'(\xi_1)} - \frac{Q_{2m}(\xi_e)}{P_{2m}(\xi_e)}] - [\frac{Q_{2m}(\xi_1)}{P_{2m}(\xi_1)} - \frac{Q_{2m}(\xi_e)}{P_{2m}(\xi_e)}]} - \frac{Q_{2m}(\xi_1)}{P_{2m}(\xi_1)} \quad . \tag{77}$$

Substituting (76) in (75) and re-arranging gives

$$\mathrm{D}_{2m}\,\sigma_5(\tau,\xi_0,\xi_1,\xi_e)-\frac{\xi_0+1}{\lambda}\frac{\sigma_3(\tau,\xi_0,\xi_1,\xi_e)D_{2m}P_{2m}'(\xi_0)+D_{2m}Q_{2m}'(\xi_0)}{2m(2\mathrm{m}+1)}$$

$$=(4m+1)\frac{\xi_0+1}{\lambda}\mathrm{D}_0\mathrm{Q}_0'(\xi_0)I_{2m}$$

which can be re-arranged into

$$\mathrm{D}_{2m}=\frac{\mathrm{D}_0(4m+1)\frac{\xi_0+1}{\lambda}\mathrm{Q}_0'(\xi_0)I_{2m}}{\sigma_5(\tau,\xi_0,\xi_1,\xi_e)-\frac{\xi_0+1}{\lambda}\frac{\sigma_3(\tau,\xi_0,\xi_1,\xi_e)P_{2m}'(\xi_0)+Q_{2m}'(\xi_0)}{2m(2\mathrm{m}+1)}}.$$

is the above can be written as

$$\mathrm{D}_{2m}=\mathrm{D}_0\,\sigma_2(\lambda,\tau,\xi_0,\xi_1,\xi_e)\ , \tag{78}$$

where

$$\sigma_2(\lambda,\tau,\xi_0,\xi_1,\xi_e)=\frac{(4m+1)\frac{\xi_0+1}{\lambda}\mathrm{Q}_0'(\xi_0)I_{2m}}{\sigma_5(\tau,\xi_0,\xi_1,\xi_e)-\frac{\xi_0+1}{\lambda}\frac{\sigma_3(\tau,\xi_0,\xi_1,\xi_e)P_{2m}'(\xi_0)+Q_{2m}'(\xi_0)}{2m(2\mathrm{m}+1)}}\ . \tag{79}$$

Equation (68) is0

$$D_0=\frac{-\Delta p-\frac{\xi_0+1}{\lambda}\sum_{m=1}^{\infty}\frac{C_{2m}P_{2m}'(\xi_0)+D_{2m}Q_{2m}'(\xi_0)}{2m(2\mathrm{m}+1)}P_{2m}(0)+\frac{\xi_0+1}{\lambda}\mathrm{D}_0\mathrm{Q}_0'(\xi_0)[2\ln 2-1]}{Q_0(\xi_0)-Q_0(\xi_1)[1-\frac{1}{\tau}]-\frac{Q_0(\xi_e)}{\tau}}$$

Substituting for C_{2m} from (76) gives

$$D_0=\frac{-\Delta p-\frac{\xi_0+1}{\lambda}\sum_{m=1}^{\infty}(\frac{\sigma_3P_{2m}'(\xi_0)+Q_{2m}'(\xi_0)}{2m(2\mathrm{m}+1)})D_{2m}P_{2m}(0)+\frac{\xi_0+1}{\lambda}\mathrm{D}_0\mathrm{Q}_0'(\xi_0)[2\ln 2-1]}{Q_0(\xi_0)-Q_0(\xi_1)[1-\frac{1}{\tau}]-\frac{Q_0(\xi_e)}{\tau}}\ .$$

Now substituting for D_{2m} in terms of D_0 gives us

$$D_0 = \frac{-\Delta p - \frac{\xi_0+1}{\lambda}\sum_{m=1}^{\infty}(\frac{\sigma_3 P_{2m}'(\xi_0)+Q_{2m}'(\xi_0)}{2m(2\mathrm{m}+1)})\mathrm{D}_0\,\sigma_2(\lambda,\tau,\xi_0,\xi_1,\xi_e)P_{2m}(0)+\frac{\xi_0+1}{\lambda}\mathrm{D}_0\mathrm{Q}_0'(\xi_0)[2\ln 2-1]}{Q_0(\xi_0)-Q_0(\xi_1)[1-\frac{1}{\tau}]-\frac{Q_0(\xi_e)}{\tau}}$$

. This is re-arranged to give

$$\mathrm{D}_0 = \frac{-\Delta p}{\sigma_1(\lambda,\tau,\xi_0,\xi_1,\xi_e)}\ , \tag{80}$$

where

$$\sigma_1(\lambda,\tau,\xi_0,\xi_1,\xi_e) = [Q_0(\xi_0)-Q_0(\xi_1)[1-\frac{1}{\tau}]-\frac{Q_0(\xi_e)}{\tau}]$$
$$+\frac{\xi_0+1}{\lambda}\sum_{m=1}^{\infty}(\frac{\sigma_3 P_{2m}'(\xi_0)+Q_{2m}'(\xi_0)}{2m(2\mathrm{m}+1)})\sigma_2(\lambda,\tau,\xi_0,\xi_1,\xi_e)P_{2m}(0)-\frac{\xi_0+1}{\lambda}\mathrm{Q}_0'(\xi_0)[2\ln 2-1]$$

. (81)

To summarize, the expressions for the coefficients are

For $m=0$:

$$\begin{aligned}
\mathrm{D}_0 &= \frac{-\Delta p}{\sigma_1(\lambda,\tau,\xi_0,\xi_1,\xi_e)}\\
C_0 &= p_e - \frac{D_0}{\tau}Q_0(\xi_e) - Q_0(\xi_1)[\mathrm{D}_0 - \frac{D_0}{\tau}]\\
B_0 &= \frac{D_0}{\tau}\\
A_0 &= p_e - \frac{D_0}{\tau}Q_0(\xi_e)
\end{aligned}\ ; \tag{82}$$

For, $m \geq 1$

$$\mathrm{D}_{2m} = \mathrm{D}_0\, \sigma_2(\lambda, \tau, \xi_0, \xi_1, \xi_e)$$

$$C_{2m} = \sigma_3(\tau, \xi_0, \xi_1, \xi_e) D_{2m}$$

$$B_{2m} = \mathrm{D}_{2m} \frac{\left[\frac{Q_{2m}'(\xi_1)}{P_{2m}'(\xi_1)} - \frac{Q_{2m}(\xi_1)}{P_{2m}(\xi_1)} \right]}{\tau \left[\frac{Q_{2m}'(\xi_1)}{P_{2m}'(\xi_1)} - \frac{Q_{2m}(\xi_e)}{P_{2m}(\xi_e)} \right] - \left[\frac{Q_{2m}(\xi_1)}{P_{2m}(\xi_1)} - \frac{Q_{2m}(\xi_e)}{P_{2m}(\xi_e)} \right]}$$

$$A_{2m} = -\frac{B_{2m} Q_{2m}(\xi_e)}{P_{2m}(\xi_e)}$$

6. Flow rate at the stele-cortex interface

The flow rate at the cortex-stele interface is calculated as

$$q_{xc} = -\mathrm{v}_{\tilde{\xi}}\,|_{\tilde{\xi}_0} \tag{83}$$

which by Darcy's law gives

$$q_{xc} = \frac{\kappa_c}{\mu}\frac{1}{L\sqrt{\sinh^2\tilde{\xi}_0 + \sin^2\tilde{\eta}}}\frac{\partial p_c}{\partial\tilde{\xi}}\,|_{\tilde{\xi}_0} = \frac{\kappa_c}{\mu}\frac{\sinh\tilde{\xi}_0}{L\sqrt{\sinh^2\tilde{\xi}_0 + \sin^2\tilde{\eta}}}\frac{\partial p_c}{\partial\xi}\,|_{\xi_0} \tag{84}$$

$$= \frac{\kappa_c}{\mu}\frac{\sqrt{\xi_0^{\,2}-1}}{L\sqrt{\xi_0^{\,2}-\eta^2}}\frac{\partial p_c}{\partial\xi}\,|_{\xi_0}\,.$$

And

$$\frac{\partial p_c}{\partial\xi}\,|_{\tilde{\xi}_0} = \sum_{m=0}^{\infty}[\mathrm{C}_{2m}P_{2m}'(\xi_0) + D_{2m}Q_{2m}'(\xi_0)]P_{2m}(\eta) \tag{85}$$

The flow rate at the cortex-stele interface is therefore

$$Q_{xc} = \int_{\tilde{\xi}_0} q_{xc}\,dA_{\tilde{\xi}_0}\ , \tag{86}$$

where $dA_{\tilde{\xi}_0}$ is the area element on the stele-cortex interface and is given by

$$dA_{\tilde{\xi}_0} = h_{\tilde{\varphi}}h_{\tilde{\eta}}\,d\tilde{\varphi}d\tilde{\eta} = L^2\sqrt{\sinh^2\tilde{\xi}_0 + \sin^2\tilde{\eta}}\,\sinh\tilde{\xi}_0\sin\tilde{\eta}\,d\tilde{\varphi}d\tilde{\eta}$$

$$= L^2\sqrt{\xi_0^{\,2}-\eta^2}\sqrt{\xi_0^{\,2}-1}\sqrt{1-\eta^2}\,d\tilde{\varphi}d\tilde{\eta}$$

Now $\eta = \cos\tilde{\eta} \Rightarrow d\eta = -\sin\tilde{\eta}\,d\tilde{\eta}$ which gives $\dfrac{d\eta}{-\sqrt{1-\eta^2}} = d\tilde{\eta}$

This gives

$$dA_{\tilde{\xi}_0} = -L^2\sqrt{\xi_0^{\,2}-\eta^2}\sqrt{\xi_0^{\,2}-1}\,d\tilde{\varphi}d\eta \tag{87}$$

Under the slender body limit, the limit $\xi_0 \to 1$ is taken and the area element is approximated to that of a perfect cylinder whose base radius is the same as that of the ellipsoid corresponding to $\tilde{\xi}_0$. This approximation gives

$$dA_{\tilde{\xi}_0} = -L^2\sqrt{\xi_0^{\,2}-1}\,d\tilde{\varphi}d\eta \tag{88}$$

The flow rate is then calculated as

$$Q_{xc} = \int_{\tilde{\eta}=0}^{\pi/2}\int_{\tilde{\varphi}=0}^{2\pi} q_{xc}\,dA_{\tilde{\xi}_0}$$

$$Q_{xc} = -\int_{\eta=1}^{0}\int_{\tilde{\varphi}=0}^{2\pi} \frac{\kappa_c}{\mu}\frac{\sqrt{\xi_0^{\,2}-1}}{L\sqrt{\xi_0^{\,2}-\eta^2}}\frac{\partial p_c}{\partial \xi}|_{\xi_0}\; L^2\sqrt{\xi_0^{\,2}-1}\,d\tilde{\varphi}d\eta$$

$$Q_{xc} = -2\pi L\frac{\kappa_c}{\mu}(\xi_0^{\,2}-1)\int_{\eta=1}^{0}\frac{1}{\sqrt{\xi_0^{\,2}-\eta^2}}\frac{\partial p_c}{\partial \xi}|_{\xi_0}\,d\eta \tag{89}$$

Once again, the slender body limit, $\xi_0 \to 1$ is employed, to re-write the above expression as

$$Q_{xc} = -2\pi L\frac{\kappa_c}{\mu}(\xi_0^{\,2}-1)\int_{\eta=1}^{0}\frac{1}{\sqrt{1-\eta^2}}\frac{\partial p_c}{\partial \xi}|_{\xi_0}\,d\eta \tag{90}$$

Now

$$\frac{\partial p_c}{\partial \xi}|_{\tilde{\xi}_0} = \sum\nolimits_{m=0}^{\infty}[\mathrm{C}_{2m}P_{2m}'(\xi_0) + D_{2m}Q_{2m}'(\xi_0)]P_{2m}(\eta)$$

$$= \mathrm{D}_0 Q_0'(\xi_0) + \sum\nolimits_{m=1}^{\infty}[\mathrm{C}_{2m}P_{2m}'(\xi_0) + D_{2m}Q_{2m}'(\xi_0)]P_{2m}(\eta)$$

Since any $P_0'(x) = 0$, this results in

$$Q_{xc} = -2\pi L \frac{\kappa_c}{\mu}(\xi_0^{\,2} - 1)\left[\begin{array}{l} \int_{\eta=1}^{0} \frac{1}{\sqrt{1-\eta^2}} \mathrm{D}_0 \, Q_0\,'(\xi_0) d\eta \\ + \int_{\eta=1}^{0} \frac{1}{\sqrt{1-\eta^2}} \sum_{m=1}^{\infty} [\mathrm{C}_{2m} \, P_{2m}\,'(\xi_0) + D_{2m} Q_{2m}\,'(\xi_0)] P_{2m}(\eta) d\eta \end{array}\right]$$

$$\begin{aligned} Q_{xc} &= 2\pi L \frac{\kappa_c}{\mu}(\xi_0^{\,2} - 1)\{\frac{\pi}{2} \mathrm{D}_0 \, Q_0\,'(\xi_0) \\ &+ \int_{\eta=0}^{1} \frac{1}{\sqrt{1-\eta^2}} \sum_{m=1}^{\infty} [\mathrm{C}_{2m} \, P_{2m}\,'(\xi_0) + D_{2m} Q_{2m}\,'(\xi_0)] P_{2m}(\eta) d\eta\} \end{aligned} . \qquad (91)$$

Q_{xc} Which can be re-arranged using (82) as

$$\begin{aligned} Q_{xc} &= 2\pi L \frac{\kappa_c}{\mu}(\xi_0^{\,2} - 1)(\frac{-\Delta p}{\sigma_1(\lambda, \tau, \xi_0, \xi_1, \xi_e)})\{\frac{\pi}{2} Q_0\,'(\xi_0) \\ &+ \int_{\eta=0}^{1} \frac{1}{\sqrt{1-\eta^2}} \sum_{m=1}^{\infty} [\sigma_3(\tau, \xi_0, \xi_1, \xi_e) P_{2m}\,'(\xi_0) + Q_{2m}\,'(\xi_0)] \sigma_2(\lambda, \tau, \xi_0, \xi_1, \xi_e) P_{2m}(\eta) d\eta\} \end{aligned} . \qquad (92)$$

7. Resistance offered by the system of the root and the soil

The resistance offered by the entire system of the root and the soil is defined as

$$R_{total} = \frac{\Delta p}{Q_{xc}} \tag{93}$$

Substituting the expression for Q_{xc} gives

$$R_{total} = \frac{-\sigma_1(\lambda,\tau,\xi_0,\xi_1,\xi_e)}{2\pi L \frac{\kappa_c}{\mu}(\xi_0^{\,2}-1)[\frac{\pi}{2}Q_0'(\xi_0) + \int_{\eta=0}^{1}\frac{1}{\sqrt{1-\eta^2}}\sum_{m=1}^{\infty}[\sigma_3(\tau,\xi_0,\xi_1,\xi_e)P_{2m}'(\xi_0)+Q_{2m}'(\xi_0)]\sigma_2(\lambda,\tau,\xi_0,\xi_1,\xi_e)P_{2m}(\eta)d\eta]} \tag{94}$$

Now, a non-dimensional resistance $\overline{R}_{total}$ is defined as

$$\overline{R}_{total} = 2\pi L \frac{\kappa_c}{\mu} R_{total}\,.$$

Then,

$$\overline{R}_{total} = \frac{-\sigma_1(\lambda,\tau,\xi_0,\xi_1,\xi_e)}{(\xi_0^{\,2}-1)\{\frac{\pi}{2}Q_0'(\xi_0) + \int_{\eta=0}^{1}\frac{1}{\sqrt{1-\eta^2}}\sum_{m=1}^{\infty}[\sigma_3(\tau,\xi_0,\xi_1,\xi_e)P_{2m}'(\xi_0)+Q_{2m}'(\xi_0)]\sigma_2(\lambda,\tau,\xi_0,\xi_1,\xi_e)P_{2m}(\eta)d\eta\}} \tag{95}$$

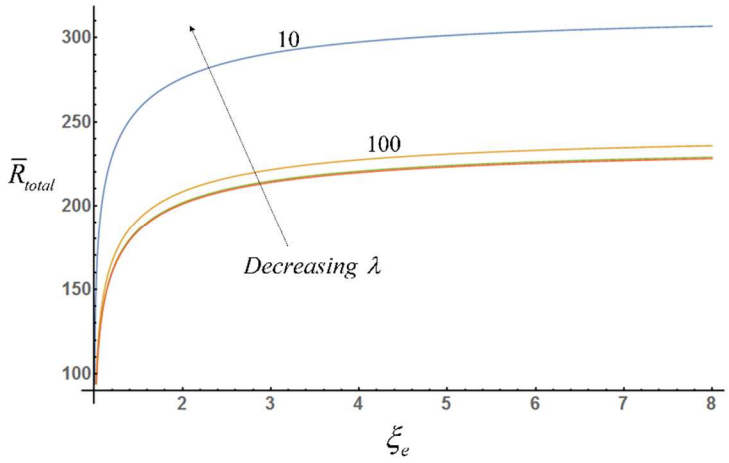

(a)

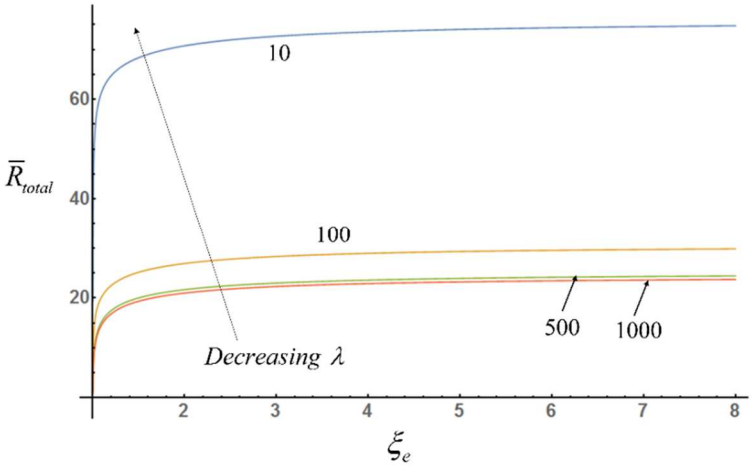

(b)

FIGURE 2. Non-dimensionalised total resistance $\overline{R}_{total}$ versus ξ_e, for $\xi_0 = 1.0005$, $\xi_0 = 1.00125$ $\lambda = 10, 100, 500, 1000$ and (a) $\tau = 0.01$ and (b) $\tau = 0.1$

This non-dimensionalized resistance is plotted against ξ_e for different parameters in Fig 2. It can be seen that the resistance increases with increasing ξ_e and reaches a constant value

with increasing ξ_e. This leveling-off occurs faster at a higher value of τ. At higher values of τ, Fig. 2(b) shows that the resistance is lower when all the other parameters are fixed. This is due to the fact that a higher τ corresponds to a higher soil permeability κ_s, which reduces resistance to water flow through the soil.

The next objective is to show that the resistance of the root and the soil system R_{total} is not equal to the sum of individual resistances of the soil R_{soil} and the root R_{root}. In order to do this, the soil resistance is determined using the method prescribed by Chen (2016); and this is discussed in detail in the following section.

8. Determination of Resistance of the Soil

The resistance of the soil is determined in a manner similar to the thermal resistance as discussed by Chen (2016). To achieve this, two constant pressure boundary conditions are imposed on both the boundaries of the soil: at $\xi = \xi_e$ and $\xi = \xi_1$. Once again, the pressure in the soil satisfies the Laplace equation and it's solution has a from similar to (30) which is

$$p_s(\xi,\eta) = \sum_{m=0}^{\infty} [\mathrm{E}_{2m}\mathrm{P}_{2m}(\xi) + F_{2m}\mathrm{Q}_{2m}(\xi)]P_{2m}(\eta) \tag{96}$$

However, due to different boundary conditions in comparison to the previous case, the co-efficients E_{2m} and E_{2m} have to be re-determined for the new boundary conditions. The new boundary conditions are

$$\xi = \xi_e; p = p_e \text{ (constant)} \tag{97}$$

$$\xi = \xi_1; p = p_1 \text{ (constant)} \tag{98}$$

This gives the equations for the co-efficients as

$$E_0 + F_0 Q_0(\xi_e) = \mathrm{p}_e \quad for \ m = 0 \tag{99}$$

$$\mathrm{E}_{2m}\mathrm{P}_{2m}(\xi_e) + F_{2m}\mathrm{Q}_{2m}(\xi_e) = 0 \quad for \quad m \geq 1 \tag{100}$$

$$E_0 + F_0 Q_0(\xi_1) = \mathrm{p}_1 \quad for \ m = 0 \tag{101}$$

$$\mathrm{E}_{2m}\mathrm{P}_{2m}(\xi_1) + F_{2m}\mathrm{Q}_{2m}(\xi_1) = 0 \quad for \quad m \geq 1 \tag{102}$$

Solving the equations (99) and (101) for $m = 0$ yields

$$F_0 = \frac{p_e - p_1}{Q_0(\xi_e) - Q_0(\xi_1)} \tag{103}$$

$$E_0 = p_1 - \frac{p_e - p_1}{Q_0(\xi_e) - Q_0(\xi_1)} Q_0(\xi_1) \tag{104}$$

For, $m \geq 1$ [from (100) and (102)]

$$\begin{bmatrix} P_{2m}(\xi_e) & Q_{2m}(\xi_e) \\ P_{2m}(\xi_1) & Q_{2m}(\xi_1) \end{bmatrix} \begin{bmatrix} E_{2m} \\ F_{2m} \end{bmatrix} = \begin{bmatrix} 0 \\ 0 \end{bmatrix} \tag{105}$$

This a matrix equation of the form $A\vec{x} = \vec{0}$. Since the determinant of matrix A is in general, non- zero for $\xi_1 \neq \xi_e$, the only possible solution is $\vec{x} = \vec{0}$.

This gives the expression for the soil pressure as

$$p_s(\xi) = \mathrm{p}_1 - \frac{p_e - p_1}{Q_0(\xi_e) - Q_0(\xi_1)} Q_0(\xi_1) + \frac{p_e - p_1}{Q_0(\xi_e) - Q_0(\xi_1)} Q_0(\xi) \tag{106}$$

The flux density entering the root through the cortex-soil interface is

$$q_{soil} = \frac{\kappa_s}{\mu} \frac{1}{L\sqrt{\sinh^2 \tilde{\xi}_1 + \sin^2 \tilde{\eta}}} \frac{\partial p_s}{\partial \tilde{\xi}} |_{\tilde{\xi}_1} = \frac{\kappa_s}{\mu} \frac{\sinh \tilde{\xi}_1}{L\sqrt{\sinh^2 \tilde{\xi}_1 + \sin^2 \tilde{\eta}}} \frac{\partial p_s}{\partial \xi} |_{\xi_1} \tag{107}$$

The flow rate is calculated as

$$Q_{soil} = \int_{\tilde{\xi}_1} q_{soil,\tilde{\xi}_1} dA_{\tilde{\xi}_1} \tag{108}$$

Where $dA_{\tilde{\xi}_1}$ is the area element on the cortex-soil interface and is given by

$$dA_{\tilde{\xi}_1} = h_{\tilde{\varphi}} h_{\tilde{\eta}} d\tilde{\varphi} d\tilde{\eta} = L^2 \sqrt{\sinh^2 \tilde{\xi}_1 + \sin^2 \tilde{\eta}} \sinh \tilde{\xi}_1 \sin \tilde{\eta} d\tilde{\varphi} d\tilde{\eta} = L^2 \sqrt{\xi_1^2 - \eta^2} \sqrt{\xi_1^2 - 1} \sqrt{1 - \eta^2} d\tilde{\varphi} d\tilde{\eta}$$

Now $\eta = \cos\tilde{\eta} \Rightarrow d\eta = -\sin\tilde{\eta}\, d\tilde{\eta}$ which gives $\dfrac{d\eta}{-\sqrt{1-\eta^2}} = d\tilde{\eta}$

Therefore

$$dA_{\tilde{\xi}_1} = -L^2\sqrt{\xi_1^2-\eta^2}\sqrt{\xi_1^2-1}\, d\tilde{\varphi}\, d\eta$$

Once again, under the slender body limit $\xi_1 \to 1$ the area element is approximated to that of a perfect cylinder whose base radius is the same as that of the ellipsoid corresponding to $\tilde{\xi}_1$. This approximation, gives

$$dA_{\tilde{\xi}_1} = -L^2\sqrt{\xi_1^2-1}\, d\tilde{\varphi}\, d\eta$$

And

$$\frac{\partial p_s}{\partial \tilde{\xi}}\Big|_{\tilde{\xi}_1} = \frac{p_e - p_1}{Q_0(\xi_e) - Q_0(\xi_1)} Q_0'(\xi_1) \tag{109}$$

The flow rate is therefore, calculated as

$$Q_{soil} = \int_{\tilde{\xi}_1} q_{soil,\tilde{\xi}_1} dA_{\tilde{\xi}_1} = -\int_{\eta=1}^{0}\int_{\tilde{\varphi}=0}^{2\pi} \frac{\kappa_s}{\mu}\frac{\sinh\tilde{\xi}_1}{\sqrt{\sinh^2\tilde{\xi}_1 + \sin^2\tilde{\eta}}}\frac{p_e - p_1}{Q_0(\xi_e) - Q_0(\xi_1)} Q_0'(\xi_1) L\sqrt{\xi_1^2-1}\, d\tilde{\varphi}\, d\eta$$

$$= 2\pi L(\xi_1^2 - 1)\frac{\kappa_s}{\mu}\frac{p_e - p_1}{Q_0(\xi_e) - Q_0(\xi_1)} Q_0'(\xi_1)\int_{\eta=0}^{1}\frac{1}{\sqrt{\xi^2{}_1 - \eta^2}}\, d\eta$$

Under the slender body limit where $\xi_1 \to 1$

$$Q_{soil} = 2\pi L(\xi_1^2 - 1)\frac{\kappa_s}{\mu}\frac{p_e - p_1}{Q_0(\xi_e) - Q_0(\xi_1)} Q_0'(\xi_1)\int_{\eta=0}^{1}\frac{1}{\sqrt{1-\eta^2}}\, d\eta$$

Which upon integration gives

$$Q_{soil} = 2\pi L(\xi_1^2 - 1)\frac{K_s}{\mu}\frac{p_e - p_1}{Q_0(\xi_e) - Q_0(\xi_1)}Q_0'(\xi_1)(\frac{\pi}{2})$$

The Resistance of the soil is given by

$$R_{soil} = \frac{p_e - p_1}{Q_{soil}} \tag{110}$$

Substituting the expression for Q_{soil} gives

$$R_{soil} = \frac{1}{2\pi L(\xi_1^2 - 1)\frac{\kappa_s}{\mu}\frac{1}{Q_0(\xi_e) - Q_0(\xi_1)}Q_0'(\xi_1)(\frac{\pi}{2})} \tag{111}$$

Employing the relation

$$Q_0'(x) = -\frac{1}{x^2 - 1}$$

simplifies the above formula to

$$R_{soil} = \frac{-1}{2\pi L\frac{\kappa_s}{\mu}\frac{1}{Q_0(\xi_e) - Q_0(\xi_1)}(\frac{\pi}{2})} \tag{112}$$

9. Resistance of the Root

The prolate spheroidal model for the Hydraulic Resistance of a single root was derived by Chen (2016). In this model, the root surface is geometrically modeled as one half of a prolate-spheroid with the base of the root located at $z = 0$ (Fig. 3). The problem is solved in alternate prolate spheroidal coordinates (ξ, η, φ) and the Cartesian coordinates (x, y, z) are related to the prolate spheroidal coordinates by

$$x = L\sqrt{\xi^2 - 1}\sqrt{1 - \eta^2}\cos\varphi, y = L\sqrt{\xi^2 - 1}\sqrt{1 - \eta^2}\sin\varphi, z = L\xi\eta, \qquad (113)$$

where $1 \le \xi < \infty, 0 \le \eta \le 1, 0 \le \varphi \le 2\pi$; L is the focal distance.(Note that the alternate prolate spheroidal co-ordinates mentioned here are related to the prolate spheroidal co-ordinates mentioned in section 2 by (9)) Here constant values of (ξ, η, φ) represent families of confocal ellipsoids, confocal hyperbolae and two-dimensional flat planes respectively. The ellipsoidal root surface is described by $\xi = \xi_1$. The interface separating the stele from the cortex vessels is modeled similarly as one half of a prolate-spheroid confocal with the root surface, $\xi = \xi_0$ ($\xi_0 < \xi_1$) and the flow in the stele is assumed to be one dimensional, along the z-axis towards the base of the root. $z_0 = L\xi_0$ is the length of the stele, and $z_1 = L\xi_1$ is the length of the root. At the base of the root, $z = 0$, the radius of the stele is $r_0 = L\sqrt{\xi_0^2 - 1}$ and the radius of the root is $r_e = L\sqrt{\xi_1^2 - 1}$ The stele core and the cortex annulus occupy the regions $1 \le \xi \le \xi_0$ and $\xi_0 \le \xi \le \xi_1$, respectively.

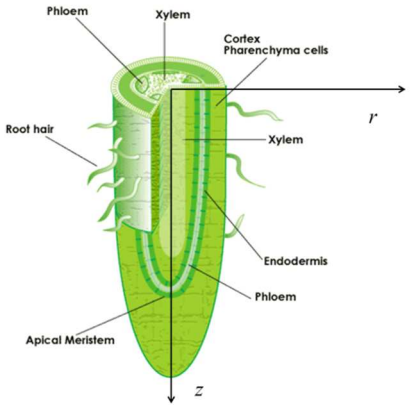

FIGURE 3. A root modeled as a composite structure of two ellipsoids. Gravity is negligible at single root scale

Under the slender-body approximation (Batchelor, 1967), the hydraulic resistance of the root is given by (Chen, 2016),

$$R_{root} = \frac{\mu}{2\pi\kappa_c L} \frac{Q_0(\xi_0) - Q_0(\xi_1) + (\xi_0 + 1)\dfrac{2\ln 2 - 1 - g(C_{sD}, \xi_0, \xi_1)}{C_{sD}}}{\dfrac{\pi}{2} - (\xi_0^2 - 1)\displaystyle\sum_{m=1}^{\infty}\left[a_{2m}P_{2m}^{'}(\xi_0) + b_{2m}Q_{2m}^{'}(\xi_0)\right]\int_0^1 \frac{P_{2m}(\sigma)}{\sqrt{1-\sigma^2}}d\sigma} \quad (114)$$

where,

$C_{sD} = \lambda(\xi_0^2 - 1)$ is known as the dimensionless root conductivity and

$$g(C_{sD}, \xi_0, \xi_1) = \sum_{m=1}^{\infty} \frac{(4m+1)(\xi_0+1)I_{2m}P_{2m}(0)}{2m(2m+1)\dfrac{C_{sD}}{\xi_0^2 - 1}\dfrac{Q_{2m}(\xi_0)P_{2m}(\xi_1) - P_{2m}(\xi_0)Q_{2m}(\xi_1)}{Q_{2m}^{'}(\xi_0)P_{2m}(\xi_1) - P_{2m}^{'}(\xi_0)Q_{2m}(\xi_1)} - (\xi_0 + 1)} \quad (115)$$

$$b_{2m} = \frac{2m(2m+1)(4m+1)(\xi_0+1)I_{2m}Q_0^{'}(\xi_0)P_{2m}(\xi_1)}{2m(2m+1)\frac{C_{sD}}{\xi_0^2-1}[Q_{2m}(\xi_0)P_{2m}(\xi_1)-P_{2m}(\xi_0)Q_{2m}(\xi_1)]-(\xi_0+1)[Q_{2m}^{'}(\xi_0)P_{2m}(\xi_1)-P_{2m}^{'}(\xi_0)Q_{2m}(\xi_1)]},$$

$$a_{2m} = -b_{2m}\frac{Q_{2m}(\xi_1)}{P_{2m}(\xi_1)}, m \geq 1.$$

(116)

The simple sum of the resistance of the soil and the root is

$$R_{soil+root} = R_{soil} + R_{root} \tag{117}$$

$$\begin{aligned} R_{soil+root} &= R_{soil} + R_{root} \\ &= \frac{-1}{2\pi L\frac{\kappa_s}{\mu}\frac{1}{Q_0(\xi_e)-Q_0(\xi_1)}(\frac{\pi}{2})} + \\ &\quad \frac{\mu}{2\pi\kappa_C L}\frac{Q_0(\xi_0)-Q_0(\xi_1)+(\xi_0+1)\frac{2\ln 2-1-\mathrm{g}(C_{sD},\xi_0,\xi_1)}{C_{sD}}}{\frac{\pi}{2}-\left(\xi_0^2-1\right)\sum_{m=1}^{\infty}\left[a_{2m}P_{2m}^{'}(\xi_0)+b_{2m}Q_{2m}^{'}(\xi_0)\right]\int_0^1\frac{P_{2m}(\sigma)}{\sqrt{1-\sigma^2}}d\sigma} \end{aligned} \tag{118}$$

Now define a non-dimensional resistance $\overline{R}_{soil+root}$ as

$$\overline{R}_{soil+root} = 2\pi L\frac{\kappa_c}{\mu}R_{soil+root}$$

Then,

$$\begin{aligned} \overline{R}_{soil+root} &= \frac{-1}{\tau\frac{1}{Q_0(\xi_e)-Q_0(\xi_1)}(\frac{\pi}{2})} \\ &\quad + \frac{Q_0(\xi_0)-Q_0(\xi_1)+(\xi_0+1)\frac{2\ln 2-1-\mathrm{g}(C_{sD},\xi_0,\xi_1)}{C_{sD}}}{\frac{\pi}{2}-\left(\xi_0^2-1\right)\sum_{m=1}^{\infty}\left[a_{2m}P_{2m}^{'}(\xi_0)+b_{2m}Q_{2m}^{'}(\xi_0)\right]\int_0^1\frac{P_{2m}(\sigma)}{\sqrt{1-\sigma^2}}d\sigma} \end{aligned} \tag{119}$$

10. Difference between R_{total} and $R_{soil+root}$

To check if the resistance of the soil-root system is the same as the sum of the resistance of the soil and the resistance of the root, a quantity R_{diff} which represents the difference is defined:

$$R_{diff} = R_{total} - R_{soil+root} \quad . \tag{120}$$

Once again, a non-dimensional resistance difference is defined as

$$\bar{R}_{diff} = 2\pi L \frac{\kappa_c}{\mu} R_{diff}$$

which gives

$$\bar{R}_{diff} = \bar{R}_{total} - \bar{R}_{soil+root} \quad . \tag{121}$$

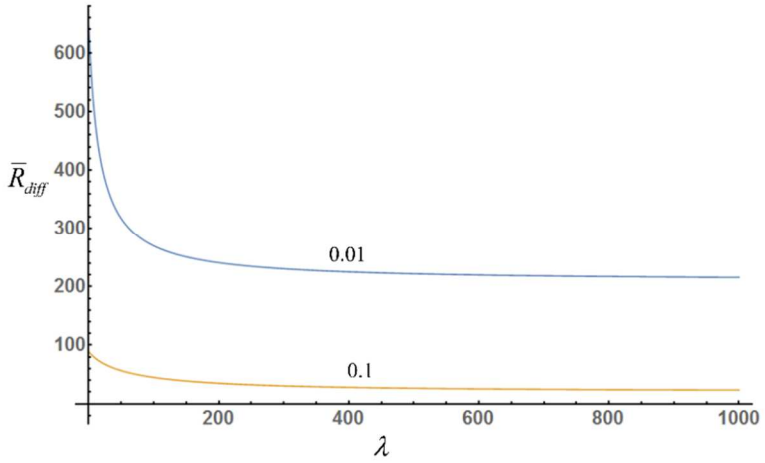

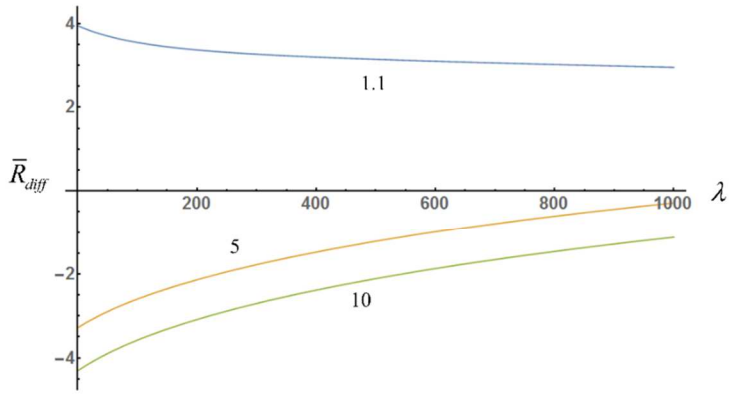

FIGURE 4. $\overline{R}_{diff}$ vs λ for $\xi_0 = 1.00005$, $\xi_1 = 1.00125$, $\xi_e = 10$ with different values of τ as shown

This difference is plotted in Fig. 4 for selected cases. These plots clearly show that, in general, the difference in resistance is non-zero, and claiming that the resistance of the soil and the root system is the simple sum of the resistances of the soil and the root can yield erroneous results. Therefore, despite having a fluid flow problem that is governed by a linear equation (Darcy's law) and linear boundary conditions, the resistance does not have a linear relationship.

This non-additivity of the resistance is due to the one-dimensional flow towards the base of the stele. Recall that while calculating the resistance of the root, a constant pressure was imposed on the cortex-soil interface. However, the solution for the complex root structure showed that the pressure along the cortex-soil surface is not unifrom. While the ellipsoids representing the stele, cortex and outer boundary are confocal, the flow field is non-confocal, with a non-uniform pressure distribution on the cortex-soil surface. This is contrast to the problem solved by Chen (2016) where a constant pressure is imposed on the root soil interface.

This non-additivity of resistance is in direct contrast to one-dimensional problems for which the resistance is an additive quantity. For one-dimensional problems, the boundary separating two different regions is a point, and the pressure, or the potential, only needs to be specified on such a single point. Thus, the resistance is the sum of the resistance of each segment. For two-dimensional problems, the boundary between two different regimes is a surface; and there is no guarantee that the potential on the boundary surface can be maintained as constant. In other words, despite of the linearity of the problem, the analogy to electric network is only appropriate for one-dimensional problems. Unfortunately, this limitation has not always been obeyed, as many work in the literature have abusively used such an analogy based on the argument of the linearity of the problem. On the other hand, this does not diminish the value of the resistance of a single root: in a macroscopic approach, the single root can be treated as a point; as such, there is no issue about the "uniform pressure" on the cortex-soil surface. Then the difference between the pressure of the soil and the pressure of the root at the same spatial location and the single root resistance can be used to compute the water-uptake of the single root at that location as $\left(p(\theta)-p_r(\mathbf{x})\right)/R$, as discussed in the Introduction section.

11. Optimum root shape for minimum hydraulic resistance

The hydraulic resistance of a root represents an intrinsic property of the root that is independent of the soil conditions. It is calculated as the ratio of pressure difference to the flow rate when a constant pressure on the cortex-soil interface is imposed. The root hydraulic resistance is given by

$$R_{root} = \frac{\mu}{2\pi\kappa_C L} \frac{Q_0(\xi_0) - Q_0(\xi_1) + (\xi_0 + 1)\dfrac{2\ln 2 - 1 - \mathrm{g}(C_{sD}, \xi_0, \xi_1)}{C_{sD}}}{\dfrac{\pi}{2} - \left(\xi_0^2 - 1\right)\displaystyle\sum_{m=1}^{\infty}\left[a_{2m}P_{2m}^{'}(\xi_0) + b_{2m}Q_{2m}^{'}(\xi_0)\right]\int_0^1 \frac{P_{2m}(\sigma)}{\sqrt{1-\sigma^2}}d\sigma} \quad (122)$$

where,

$C_{sD} = \lambda(\xi_0^2 - 1)$ is known as the dimensionless root conductivity and

$$g(C_{sD}, \xi_0, \xi_1) = \sum_{m=1}^{\infty} \frac{(4m+1)(\xi_0+1)I_{2m}P_{2m}(0)}{2m(2m+1)\dfrac{C_{sD}}{\xi_0^2 - 1}\dfrac{Q_{2m}(\xi_0)P_{2m}(\xi_1) - P_{2m}(\xi_0)Q_{2m}(\xi_1)}{Q_{2m}^{'}(\xi_0)P_{2m}(\xi_1) - P_{2m}^{'}(\xi_0)Q_{2m}(\xi_1)} - (\xi_0+1)}$$

$$b_{2m} = \frac{2m(2m+1)(4m+1)(\xi_0+1)I_{2m}Q_0^{'}(\xi_0)P_{2m}(\xi_1)}{2m(2m+1)\dfrac{C_{sD}}{\xi_0^2-1}[Q_{2m}(\xi_0)P_{2m}(\xi_1) - P_{2m}(\xi_0)Q_{2m}(\xi_1)] - (\xi_0+1)[Q_{2m}^{'}(\xi_0)P_{2m}(\xi_1) - P_{2m}^{'}(\xi_0)Q_{2m}(\xi_1)]},$$

$$a_{2m} = -b_{2m}\frac{Q_{2m}(\xi_1)}{P_{2m}(\xi_1)}, m \geq 1.$$

The volume of the entire root, given by the volume of the ellipsoid representing the cortex-soil surface is

$$V_1 = \frac{2}{3}\pi x_1 {z_1}^2 \quad (123)$$

where x_1 is length of the semi-major axis of the ellipsoid and z_1 is the base radius or length of semi-minor axis of the ellipsoid and are given by

$$x_1 = L\xi_1$$
$$z_1 = L(\xi_1^2 - 1)^{1/2} \tag{124}$$

Substituting (124) in (123) gives

$$V_1 = \frac{2}{3}\pi L^3 \xi_1 (\xi_1^2 - 1)\,. \tag{125}$$

Thus,

$$L = \left(\frac{3V_1}{2\pi} \frac{1}{\xi_1(\xi_1^2 - 1)} \right)^{1/3}\,. \tag{126}$$

Therefore, the expression for resistance can be re-written as

$$R_{root} = \frac{\mu}{2\pi\kappa_C \left(\frac{3V_1}{2\pi} \frac{1}{\xi_1(\xi_1^2 - 1)} \right)^{1/3}} \frac{Q_0(\xi_0) - Q_0(\xi_1) + (\xi_0 + 1)\frac{2\ln 2 - 1 - \mathrm{g}(C_{sD}, \xi_0, \xi_1)}{C_{sD}}}{\frac{\pi}{2} - (\xi_0^2 - 1)\sum_{m=1}^{\infty}\left[a_{2m} P_{2m}^{'}(\xi_0) + b_{2m} Q_{2m}^{'}(\xi_0) \right] \int_0^1 \frac{P_{2m}(\sigma)}{\sqrt{1-\sigma^2}} d\sigma}$$

$$= \frac{\mu}{2\pi\kappa_C \left(\frac{3V_1}{2\pi} \right)^{1/3}} * J(C_{sD}, \xi_0, \xi_1) \tag{127}$$

where

$$J(C_{sD}, \xi_0, \xi_1) = \frac{1}{\left(\frac{1}{\xi_1(\xi_1^2 - 1)} \right)^{1/3}} * \frac{Q_0(\xi_0) - Q_0(\xi_1) + (\xi_0 + 1)\frac{2\ln 2 - 1 - \mathrm{g}(C_{sD}, \xi_0, \xi_1)}{C_{sD}}}{\frac{\pi}{2} - (\xi_0^2 - 1)\sum_{m=1}^{\infty}\left[a_{2m} P_{2m}^{'}(\xi_0) + b_{2m} Q_{2m}^{'}(\xi_0) \right] \int_0^1 \frac{P_{2m}(\sigma)}{\sqrt{1-\sigma^2}} d\sigma} \tag{128}$$

The ellipsoidal co-ordinate, ξ_1 that represents the cortex-soil interface can also be expressed as the length-to-base radius ratio of the entire composite root. First define a length-to-base radius ratio as

$$l_1 = \frac{x_1}{z_1} = \frac{\xi_1}{\sqrt{\xi_1^2 - 1}} \ . \tag{129}$$

Thus ξ_1 is given by

$$\xi_1 = \frac{1}{\sqrt{1 - \frac{1}{l_1^2}}} \tag{130}$$

Next, a parameter β is defined, that represents the ratio of base radius of the stele to the base radius of the root:

$$\beta = \frac{\sqrt{\xi_0^2 - 1}}{\sqrt{\xi_1^2 - 1}} < 1 \tag{131}$$

In the following section, the dependence of resistance on the shape of the root is discussed.

11.1 Dependence of resistance on l_1 for constant C_{sD}

From (123) to (131), it can be noted that by fixing the volume V_1 of the root and fixing the parameters C_{sD}, μ, κ_c and β, allows the study of dependence of the resistance on the geometric parameter l_1, by studying the function $J(l_1, C_{sD}, \beta)$.

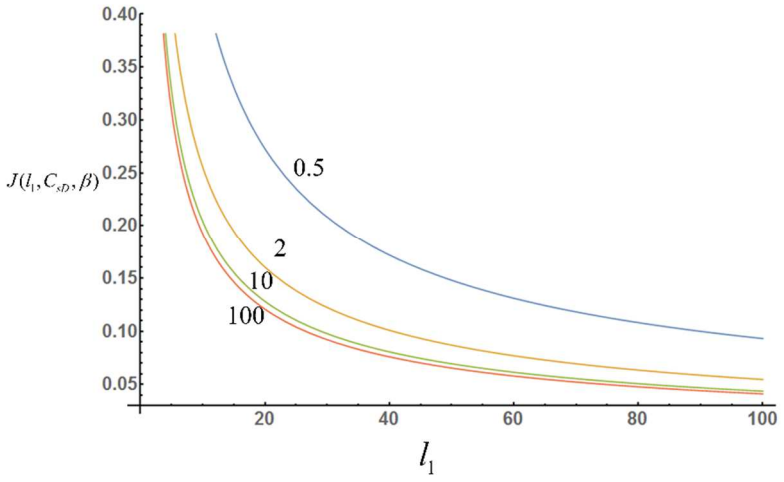
0.40
0.35
0.30
0.25
0.20
0.15
0.10
0.05
$J(l_1, C_{xD}, \beta)$
0.5
2
10
100
20
40
60
80
100
l_1

(a)

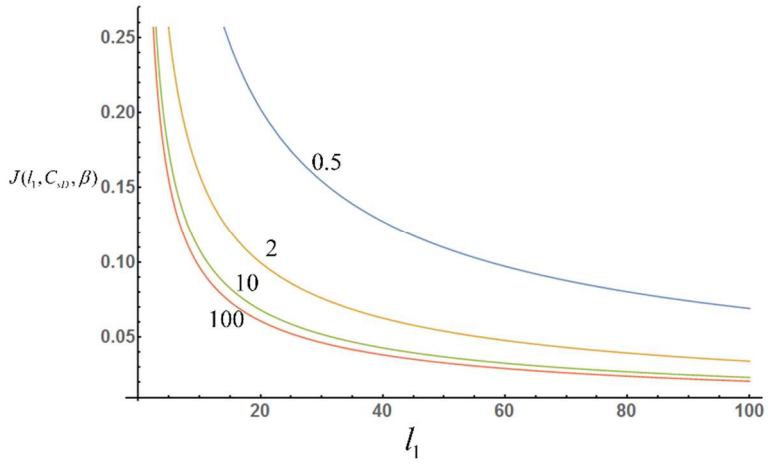
0.25
0.20
0.15
0.10
0.05
$J(l_1, C_{xD}, \beta)$
0.5
2
10
100
20
40
60
80
100
l_1

(b)

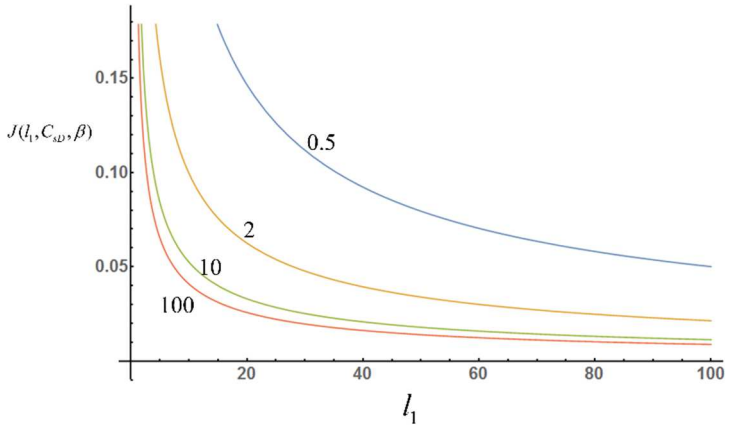

(c)

FIGURE 5. $J(l_1, C_{sD}, \beta)$ vs l_1 for different values of C_{sD} as shown in the figure

(a) $\beta = 0.25$ (b) $\beta = 0.5$ (c) $\beta = 0.75$

From Fig. 5, it can be seen that for a fixed value of C_{sD} and β, the resistance decreases with increase in the root length-to-base radius ratio l_1. This can be understood by equations (130) and (131) and the definition of C_{sD}, which is

$$C_{sD} = \lambda(\xi_0^2 - 1) \ . \tag{132}$$

It can be seen from (130) and (131) that increasing l_1 causes a decrease in both ξ_0 and ξ_1 and therefore, an increase in λ according to (132), since C_{sD} is fixed. Therefore, increasing l_1 leads to a thinner or more 'slender' root. This decrease of ξ_0 has two consequences for the flow rate at the base of the stele. It increases the inverse square root singularity of the pressure gradient at the tip of the stele (Chen, 2015 and Chen, 2016), which significantly increases the velocity of the flow in stele. On the other hand, it also causes a reduction in

the cross-sectional area at the base of the stele (represented by $(\xi_0^2 - 1)$), which reduces the area available for water uptake. However, the requirement of a constant C_{sD} requires that λ to increase as the inverse of $(\xi_0^2 - 1)$ according to (132). Therefore any contribution of the decreased base area in reducing the flow rate (or increasing resistance) is exactly cancelled out by the increase in λ. Therefore, the increase in velocity due to the increased pressure gradient causes the resistance to decrease with increasing l_1.

11.2 Dependence of resistance on l_1 for constant λ

Further insights can be gained into the dependence of resistance on root shape by substituting C_{sD} in (132) in (128) to study the function *J* and therefore the resistance as a function of λ. This allows separation of the effect of λ from the geometry of the root.

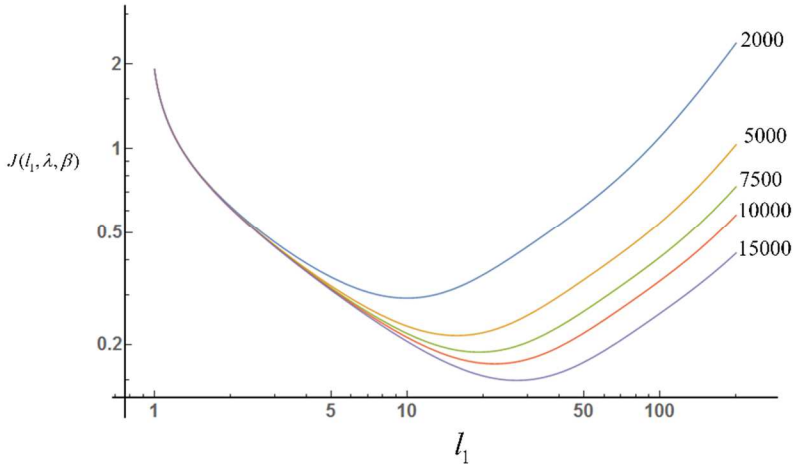

(a)

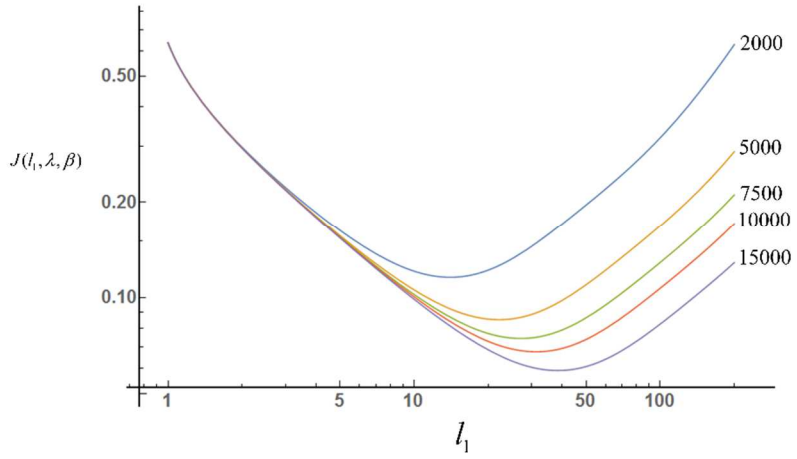

(b)

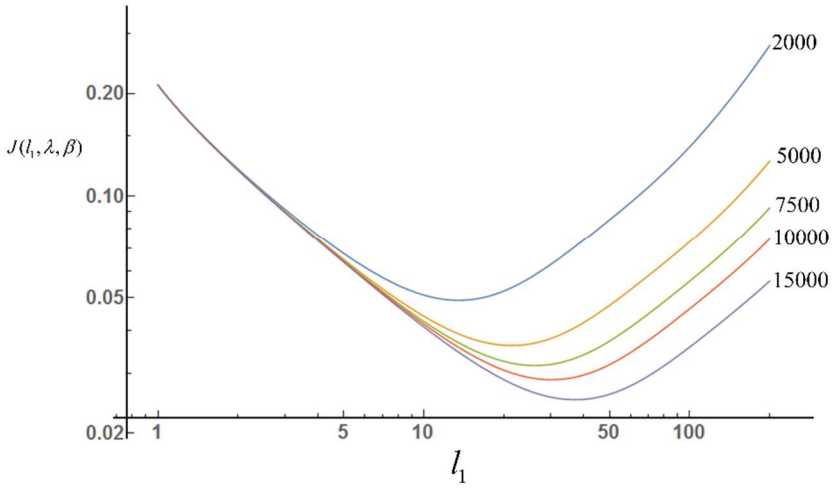

(c)

FIGURE 6. Log-Log plot of $J(l_1,\lambda,\zeta)$ vs l_1 for different values of λ as shown (a) $\beta = 0.25$ (b) $\beta = 0.5$ (c) $\beta = 0.75$

It is observed from Fig. 6 that, in general, the resistance decreases when the stele-to-cortex permeability ratio λ is increased. Furthermore, for any given permeability ratio, there is a minimum resistance at an optimum value of length-to-radius ratio l_1. As discussed

previously, an increase in l_1 causes a corresponding decrease in ξ_0 and ξ_1, which increases the 'slenderness' of the spheroid and enhances the tip singularity (Chen, 2015 and Chen, 2016), while decreasing the area available for water uptake at the base. While the tip singularity is present for all values of λ, it is important to note that the limitation of a constant λ is imposed and not one of constant C_{sD}. Therefore the two effects of decreasing ξ_0 compete to alter the resistance, while λ being constant, does not affect the behavior. An optimum 'slenderness' or length-to-base radius ratio of the root exists, where the resistance is minimum (see Fig. 6). This minimum is seen for both low and high values of stele-to-cortex base radius ratio β.

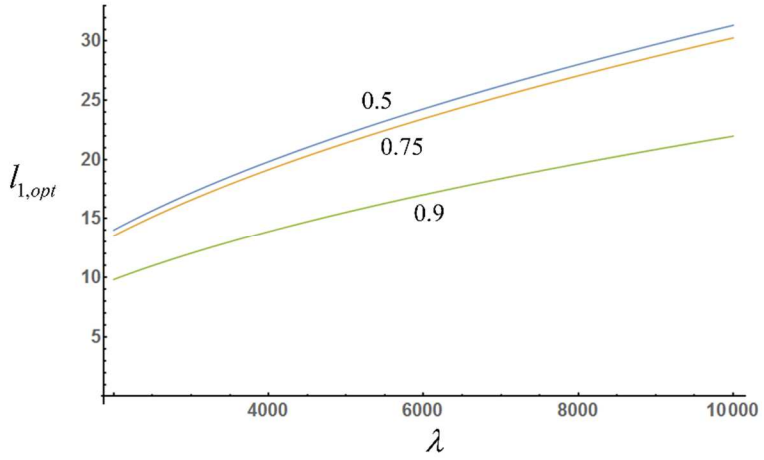

FIGURE 7. $l_{1,opt}$ vs λ at for different values of β as shown

Fig 7. shows the optimum length-to-base radius ratio $l_{1,opt}$ against λ. The optimum length-to-base radius ratio $l_{1,opt}$ increases with λ. This can be understood from the discussion above, where an increase in the stele-to-cortex permeability ratio λ allows for increased shrinking of the root size and therefore corresponds to a higher optimum value

of l_1. It is possible to find a $\xi_{0,opt}$ for a given value of $l_{1,opt}$, given value of λ and β from (130) and (131). An optimum C_{sD} is defined as

$$C_{sD,opt} = \lambda(\xi_{0,opt}^2 - 1) \ . \tag{133}$$

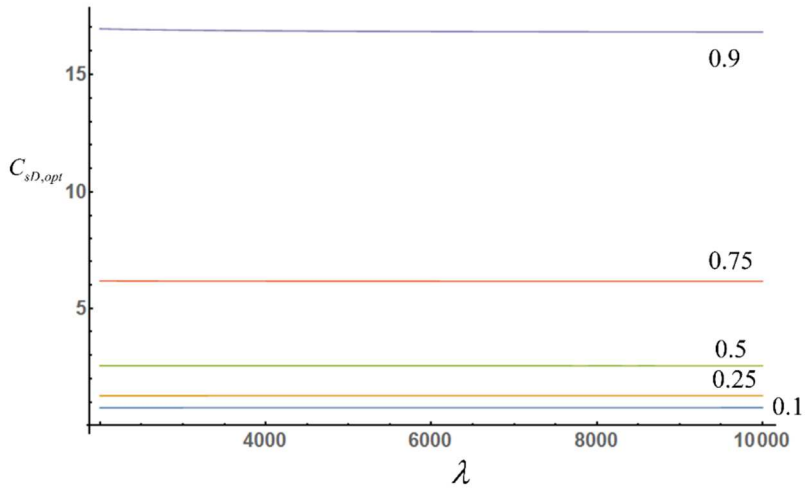

FIGURE 8. $C_{sD,opt}$ versus λ for different values of β as shown.

$C_{sD,opt}$ versus λ for different values of β is plotted in Fig. 8. It is seen that for a fixed value of β, $C_{sD,opt}$ remains constant irrespective of the value of λ. Therefore, the optimum shape for minimum resistance can be collapsed down to a dependence of $C_{sD,opt}$ on a single parameter β. Fig 8 shows a plot of $C_{sD,opt}$ against β. $C_{sD,opt}$ increases with β at a very slow rate at low values of β, while the rate of increase is much higher at higher β values. This curve applies to any value of the stele-to-cortex permeability ratio λ.

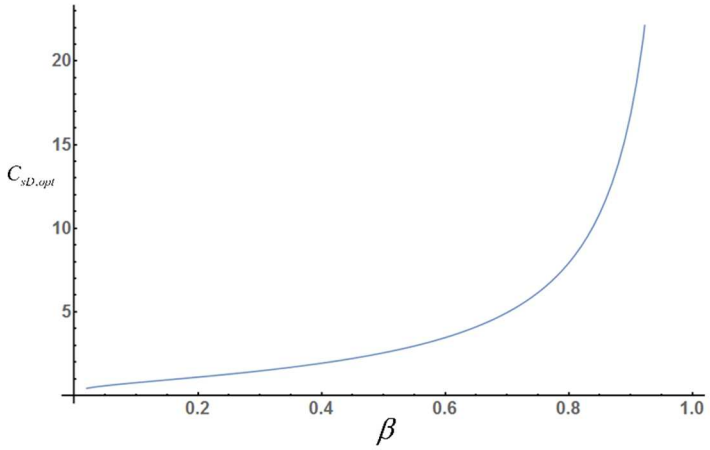

FIGURE 9. $C_{sD,opt}$ versus β

Therefore, in order to minimize the resistance for a given value of the base radius ratio β, it has to be ensured that the value of $C_{sD,opt}$ is appropriately chosen according to Fig 9. Upon choosing this, any combination of λ and $\xi_{0,opt}$ that give the corresponding value of $C_{sD,opt}$ will minimize the resistance. Physically, increasing λ decreases the resistance of the stele; while decreasing ξ_0 has two effects: it increases the slenderness of the stele, thus enhancing the pressure gradient singularity at the tip, leading to an increased velocity in the stele; On the other hand, it decreases the base radius of the stele and therefore the area available at the base for water uptake. The optimum value of ξ_0 for minimizing resistance can be determined from (133).

12. General Results for Optimal Root Shape

12.1 Physical Justification of the cylindrical area approximation

The formula for the hydraulic resistance of the composite root that was used in sections 11 and 12 was derived by Chen (2016) as

$$R_{root} = \frac{\Delta p_{root}}{Q_{root}} \tag{134}$$

Where Δp_{root} is the difference between a constant pressure imposed on the cortex-soil interface (p_1) and the pressure at the base of the stele (p_w), and the flow rate of the composite root system is

$$Q_{root} = \frac{2\pi L \kappa_C}{\mu}(\xi_0^2 - 1)\left\{\frac{\pi}{2} B'_0 Q_0'(\xi_0) + \sum_{m=1}^{\infty}\left[A'_{2m} P_{2m}'(\xi_0) + B'_{2m} Q_{2m}'(\xi_0)\right]\int_0^1 \frac{P_{2m}(\sigma)}{\sqrt{1-\sigma^2}} d\sigma\right\} \tag{135}$$

Where

$$B'_{2m} = \frac{2m(2m+1)(4m+1)(\xi_0+1) I_{2m} Q_0'(\xi_0) P_{2m}(\xi_1)}{2m(2m+1)\lambda[Q_{2m}(\xi_0)P_{2m}(\xi_1) - P_{2m}(\xi_0)Q_{2m}(\xi_1)] - (\xi_0+1)[Q_{2m}'(\xi_0)P_{2m}(\xi_1) - P_{2m}'(\xi_0)Q_{2m}(\xi_1)]} B'_0 \tag{136}$$

$$A'_{2m} = -B'_{2m}\frac{Q_{2m}(\xi_1)}{P_{2m}(\xi_1)}, m \geq 1 \tag{137}$$

$$B'_0 = -\frac{\xi_0^2 - 1}{H(\lambda, \xi_0, \xi_1)}\Delta p_{root} \tag{138}$$

$$H(\lambda, \xi_0, \xi_1) = (\xi_0^2 - 1)(Q_0(\xi_0) - Q_0(\xi_1)) + (\xi_0 + 1)\frac{2\ln 2 - 1 - g(\lambda, \xi_0, \xi_1)}{\lambda} \tag{139}$$

$$g(\lambda, \xi_0, \xi_1) = \sum_{m=1}^{\infty} \frac{(4m+1)(\xi_0+1) I_{2m} P_{2m}(0)}{2m(2m+1)\lambda \frac{Q_{2m}(\xi_0)P_{2m}(\xi_1) - P_{2m}(\xi_0)Q_{2m}(\xi_1)}{Q_{2m}'(\xi_0)P_{2m}(\xi_1) - P_{2m}'(\xi_0)Q_{2m}(\xi_1)} - (\xi_0+1)} \tag{140}$$

Note that the formula for the flow rate of a composite root system given by (135) has the same form as (91) for Q_{xc} with the only difference being the coefficients of the Legendre Polynomials.

For the derivation of Q_{root}, Chen (2016) employs the slender body approximation to replace the surface area of the stele with the surface area of a cylinder of the same length and base radius as the stele. (This is the same method employed in deriving (91) for Q_{xc}). The flow rate is given by

$$Q_{root} = \int_0^1 q_s(\eta)\, A_\xi\Big|_{\xi=\xi_0, d\eta=1}\, d\eta \tag{141}$$

where $q_s(\eta)$ is the flux density at the stele cortex interface (eq. (32) in the work of Chen(2016)) given by

$$q_s(\eta) = \frac{\kappa_C}{\mu}\frac{1}{L}\sqrt{\frac{\xi_0^2-1}{1-\eta^2}}\left\{B'_0\, Q_0^{'}(\xi_0) + \sum_{m=1}^{\infty}\left[A'_{2m}\, P_{2m}^{'}(\xi_0) + B'_{2m}\, Q_{2m}^{'}(\xi_0)\right]P_{2m}(\eta)\right\} \tag{142}$$

And $A_\xi\Big|_{\xi=\xi_0, d\eta=1}$ is the area per unit increment of η on the stele cortex interface, under the slender body approximation of an equivalent cylinder (eq. (33) in the work of Chen(2016)) and is given by

$$A_\xi\Big|_{\xi=\xi_0, d\eta=1} \to 2\pi r_0 L = 2\pi L^2\sqrt{\xi_0^2-1} \tag{143}$$

(142) and (143) are then substituted into (141) to obtain the flow rate Q_{root} which results in the formula given in (135). The model for the composite root derived by Chen (2016) assumes the existence of a hydraulic dead zone close to the tip of the root. As explained in the work of Chen (2016), this is based on the findings of Frensch & Steudle (1989), who

experimentally found that the axial conductivity of the xylem decreases from a constant value to zero within a short distance to the tip. The cone-shaped tip region requires the radius of all xylem vessels to shrink to zero in the region. Therefore, the anatomy of the root makes the tip region not "functional" for water uptake; and a root's water-uptake is accomplished only by the portion of the root behind the tip region, which has nearly constant radii for both the root outer surface and the stele. Therefore, the physical root is replaced by an equivalent mathematical root of same base radius, but of shorter length, whose surface is porous and allows for water to enter. Under the slender body limit, both the physical and mathematical root become equivalent and this justifies the use of slender body approximation for the surface area of the stele. This idea is illustrated in the figure below.

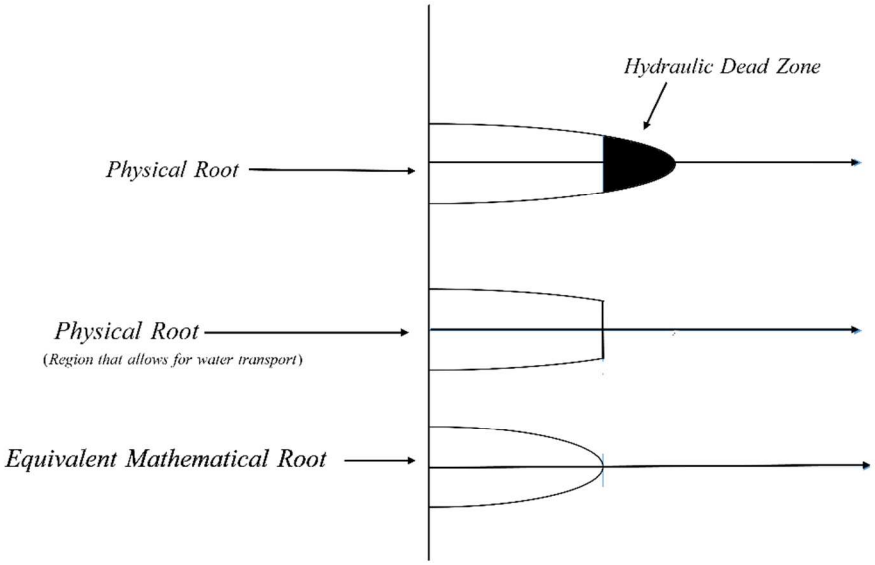

FIGURE 10. Schematics of Mathematical and Physical root geometries

Upon neglecting the hydraulic dead zone in the physical root, it can be seen that the resultant shape can be closely approximated by a cylinder that has the same base radius as the root. (The above figure is not to scale with the physical dimensions of the root, and is only for illustration). As discussed by Chen (2016), despite the presence of a hydraulic dead zone, there will always be a flux singularity as the flow converges close to the tip region. The equivalent mathematical root that is modelled to solve for the flow field and compute the resistance has the same base radius as the physical root but is of shorter length, in comparison to the ellipsoid representing the physical root. However, it fails to capture the actual area of the physical root. Thus, it seems reasonable to apply the slender body approximation to approximate the area.

12.2. Hydraulic resistance without cylindrical area approximation

If the slender body approximation is not used and the flow rate entering the stele is computed without approximating the surface area of the stele as that for a cylinder, a different hydraulic resistance formula results (this result can also be inferred from Chen, 2015),

$$\hat{R} = \frac{\mu}{2\pi L \kappa_C} \frac{H(\lambda, \xi_0, \xi_1)}{\xi_0^2 - 1} \ , \tag{144}$$

$$H(\lambda, \xi_0, \xi_1) = (\xi_0^2 - 1)(Q_0(\xi_0) - Q_0(\xi_1)) + (\xi_0 + 1)\left(2\ln 2 - 1 - \mathrm{g}(\lambda, \xi_0, \xi_1)\right)/\lambda \ . \tag{145}$$

For a specified root volume V_1 , the hydraulic resistance $\hat{R}$ can be written as

$$\hat{R} = \frac{\mu \hat{J}(C_{sD}, \xi_0, \xi_1)}{2\pi\kappa_C \left(\frac{3V_1}{2\pi}\right)^{1/3}} , \tag{146}$$

where

$$\hat{J}(\lambda, \xi_0, \xi_1) = \left(\xi_1(\xi_1^2 - 1)\right)^{1/3} H(\lambda, \xi_0, \xi_1) / (\xi_0^2 - 1) . \tag{147}$$

The same optimization strategy can be used to minimize the hydraulic resistance $\hat{R}$. The results are similar to those discussed in the previous section. Once again, the optimum stele conductivity $C_{sD,opt}$ depends only on the base-radius ratio β (Fig. 11). The values of $C_{sD,opt}$, however, are smaller than those under slender body approximation. The curve $C_{sD,opt}$ vs β is given in Fig. 12.

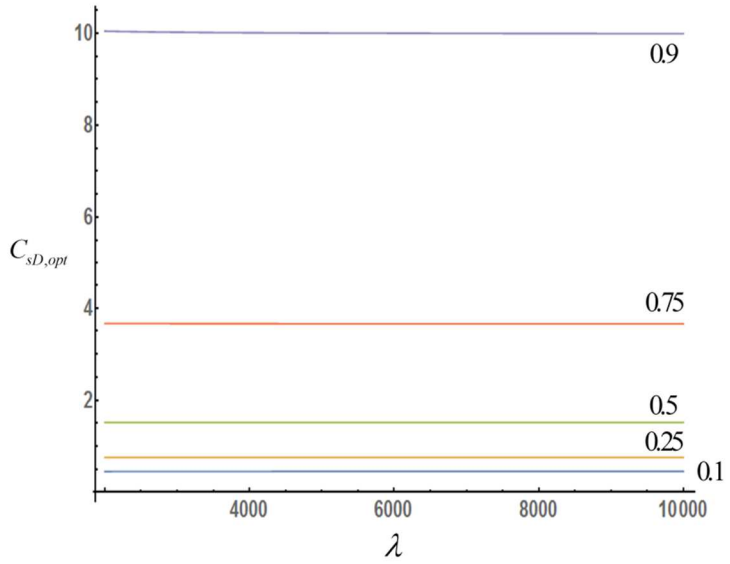

FIGURE 11. $C_{sD,opt}$ versus λ for different values of β for $\hat{R}$

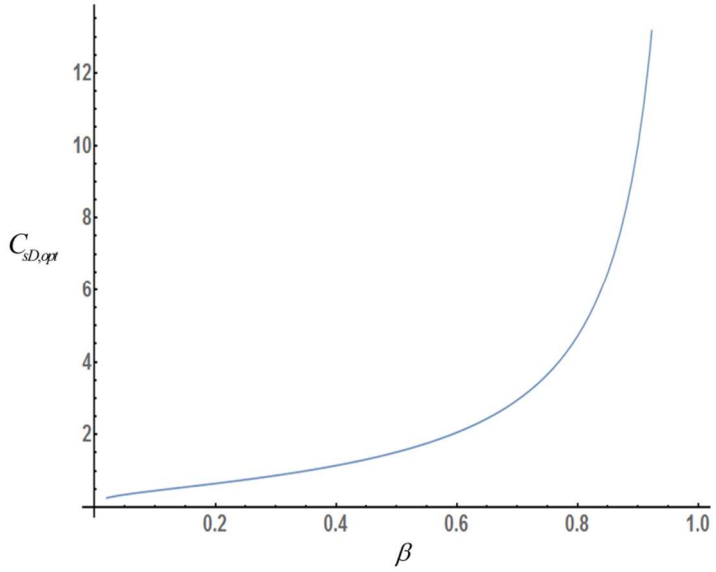

FIGURE 12. $C_{sD,opt}$ versus β for $\hat{R}$

13. Conclusion

Analytical solution for flow-field in a composite root coupled with soil is presented and an expression for the combined resistance of the soil and root system has been derived using the slender body theory. It is shown that, in general, the individual resistances of the root and soil are not linearly additive and this non-linearity was due to the non-confocal terms in the problem. This result can play a key role in future modelling of water uptake, since the resistance R is a key term that is used to calculate the volumetric sink term S in Richard's equation and this non-linearity has to be appropriately considered.

The dependence of hydraulic resistance of the root, on the shape of the root was studied. At values of constant dimensionless root conductivity, it was found that the resistance decreases continuously with increase in slenderness of the root. This intrinsic property of the root was found to have a minimum at some optimum value of root length to base radius ratio at values of constant permeability ratio λ . And when translated in terms of C_{sD} , the optimum value of C_{sD} is independent of λ , and depends on the ratio of stele radius to root radius β .

The physical justification for the slender body approximation of the stele surface by a cylinder is discussed. The flow rate of the composite root system was also calculated without the approximation. The slender body approximation always predicts a constant enhancement of the flow rate. Upon avoiding this approximation, however, it is shown that the enhancement of flow rate exists only at higher values of ξ_1 , while at lower values, the enhancement is close to zero.

REFERENCES

Batchelor, G. K. 1967 *An Introduction to Fluid Dynamics*. Cambridge Univ. Press, Cambridge, UK.

Chen, K. P., 2015 Fluid extraction from porous media by a slender semi prolate-spheroid: end-effect and shape optimization. *Extreme Mech. Ltr.* **4,** 124-130.

Chen, Kang Ping 2016 Hydraulic resistance of a plant root to water-uptake: a slender-body theory. *Journal of Theoretical Biology,* **396**, 63–74.

Chen, K. P., Jin, Y. & Chen, M. 2013 Pressure-gradient singularity and production enhancement for hydraulically-fractured wells, *Geophysical J. Intl.* **195**, 923-931.

Cowan, I. R. 1965 Transport of water in the soil-plant-atmosphere system, *J. Appl. Ecol.* **2**, 221-239.

Doussan, C., Vercambre, G. & Pages, L. 1998 Modeling of the hydraulic architecture of root systems: an integrated approach to water absorption-distribution of axial and radial conductances in maize, *Ann. Bot.,* **81**, 225-232.

Frensch, J. & Steudle, E., 1989 Axial and Radial Hydraulic Resistance to Roots of Maize (Zea mays L.), *Plant Physiol*., **91**, 719–726.

Gardner, W. R. 1960 Dynamic aspects of water availability to plants, *Soil Sci.,* **89**, 63-73.

Hainsworth, J. M. & Aylmore, L.A.G. 1986 Water extraction by single plant roots, *Soil Sci. Soc. Am. J.* **50**, 841-848.

Landsberg, J. J. & Fowkes, N. D. 1978 Water movement through plant roots, *Ann. Bot*., **42**, 493-508.

Molz, F. J. 1981 Models of water transport in the soil-plant system, *Water Resour. Res*., **17**, 1245-1260.

Passioura, J. B. 1988 Water Transport in and to roots, *Ann. Rev. Plant Physiol. Plant Mol. Biol.* **39**, 245-265.

Philip, J. R. 1957 The physical principles of soil water movement during the irrigation cycle, In: *Proc. Intern. Congr. Irrigation and Drainage*, 3rd, San Francisco, **8**,125-154.

Raats, P.A.C. 2007 Uptake of water from soils by plant roots, *Transp. Porous Med*. **68**, 5-28.

Roose, T. & Schnepf, A. 2008 Mathematical models for plant-soil interaction, *Phil. Trans. R. Soc. A*, **366**, 4597-3611.

Steudle, E. 2000 Water uptake by plant roots: an integration of views, *Plant. Soil*, **226**, 45–56.

Steudle, E. & Peterson, C. A. 1998 How does water get through roots? *J. Experiment. Botany*, **49**, 775–788.

Stroock, A.D., Pagay, V. V., Zwieniecki, M. A. & Holbrook, N. M. 2014 The Physicochemical Hydrodynamics of Vascular Plants. *Ann. Rev. Fluid Mech.***46**, 615-642.